JAERI-M
90-190

STUDY ON THERMAL PERFORMANCE OF VERTICAL GRAVITY-ASSISTED HEAT PIPES FOR IRRADIATION CAPSULES

November 1990

Manchang LI*, Haruhiko ITO, Tadao SIRAISHI, Takashi SAITO
Hiroo AMEZAWA, Yukio ITABASHI and Yoshinori ICHIHASHI

日本原子力研究所
Japan Atomic Energy Research Institute

JAERI-Mレポートは，日本原子力研究所が不定期に公刊している研究報告書です。
入手の問合わせは，日本原子力研究所技術情報部情報資料課（〒319-11 茨城県那珂郡東海村）あて，お申しこみください。なお，このほかに財団法人原子力弘済会資料センター（〒319-11 茨城県那珂郡東海村日本原子力研究所内）で複写による実費領布をおこなっております。

JAERI-M reports are issued irregularly.
Inquiries about availability of the reports should be addressed to Information Division Department of Technical Information, Japan Atomic Energy Research Institute, Tokaimura, Naka-gun, Ibaraki-ken 319-11, Japan.

編集兼発行　日本原子力研究所
印　　刷　ニッセイエブロ株式会社

JAERI-M 90-190

Study on Thermal Performance of Vertical Gravity-Assisted Heat Pipes for Irradiation Capsules

Manchang LI*, Haruhiko ITO, Tadao SIRAISHI, Takashi SAITO
Hiroo AMEZAWA, Yukio ITABASHI and Yoshinori ICHIHASHI

Department of JMTR Project
Oarai Research Establishment
Japan Atomic Energy Research Institute
Oarai-machi, Higashiibaraki-gun, Ibaraki-ken

(Received October 4, 1990)

The heat pipe has widely been used in various fields for many years. In order to use it for controlling temperature of the irradiation capsules in the JMTR, the thermal performance calculations for the wickless, the grooved and the homogeneous mesh wicked heat pipes in the vertical gravity-assisted mode were made. The calculated results prove that the former two are preferable to be used at the high working temperatures (over 200°C) and the last one is better for being used at the low temperatures (below 120°C).

All the calculated results, some analyses and discussions are presented in this report.

Keywords: Heat-pipe, Irradiation Facility, Capsule, Heat-transfer, JMTR

* Southwest Centre for Reactor Engineering Research and Design (China)

JAERI－M 90－190

キャプセル用サーモサイフォン型ヒートパイプの計算評価

日本原子力研究所大洗研究所材料試験炉部
李　　満昌*・伊藤　治彦・白石　忠男・齋藤　　隆
雨沢　博男・板橋　行夫・市橋　芳徳

（１９９０年10月４日受理）

ヒートパイプは様々な分野で長年利用されている。ＪＭＴＲにおける照射キャプセルの温度制御にヒートパイプを使用するのに当たって，ウィック無しヒートパイプと溝付きウィック及び金網ウィック付きヒートパイプを重力補助の運転モードで使用した場合の熱的特性の計算を行った。計算結果前２者，すなわちウィック無しと溝付きウィック有りヒートパイプは200℃以上の高温で有効であり，金網ウィック付きヒートパイプの場合，120℃以下の低温で有効であることが分かった。

本報告書では，キャプセル用ヒートパイプの熱的特性計算結果とその評価について報告する。

大洗研究所：〒311－13　茨城県東茨城郡大洗町成田町字新堀３６０７
＊西南反応堆工程研究設計院

Contents

目　　次

1. Introduction

The heat pipe is a device for efficiently transmitting heat along the pipe axis over a small temperature gradient. It has been well developed and widely used in many fields since the idea of the heat pipe was first put forward by R.S. Gaugler in 1942. It has also been employed in nuclear reactors for cooling irradiation capsules and controlling specimen temperatures.

In the development of irradiation technology in material testing reactors, an important consideration is the capsule design for material and fuel tests. One major problem is establishing a desired, uniform temperature on the specimens which remains constant over the duration of operation. However, it is quite difficult and sometimes impossible to achieve the goal because of the high uneven heat generation distribution caused by radiation. The general method used for an attempt to establish a desired material test temperature is to adopt an electric heater and vacuum (or mixed gases) control. The requested temperature can be obtained by changing the heater power and adjusting the vacuum (or mixed ratio of gas), furthermore, varing the thermal conductivity of the gas gap around the specimen capsule. The method, however, is not applicable to be used for the capsules in the core region where the gamma heat generation is very high, about 5 ~ 10 W/g, because the great amount of heat can not be removed out from the capsule through the gas gap. Fortunately, use of the heat pipe allows the problems to be solved through its high heat transfer performance, uniform temperature distribution and excellent temperature controlled capability. In recent years, the wide investigation on heat pipe technology has been carried out and the out-of-pile thermal performance tests for several types of heat pipes have been conducted in Oarai Research Establishment of JAERI to develop a high performance heat pipe which can be be used in the center of the reactor core. It is expected that in the near future a new heat pipe with a high heat-transported performance and a excellent temperature-controlled capability will be used in the irradiation capsules in the JMTR.

The typical capsule in the JMTR is shown in Fig. 1. A standard capsule consists of a stainless steel container of 40 mm in outdiameter and about 800 mm in length. The gamma heat generation rate is 10 W/g in the center of the core. The total heat generation of a capsule amounts to

about 30 kW. The capsule is cooled by primary coolant of the JMTR that flows downwards along the outer surface of the capsule.

Usually, the irradiation temperature range of the capsules is basically determined by design of the annular gas gap between the samples and the container. The temperature of samples is controlled by adjusting the pressure in the gas gap. In the case, the radiation distribution results in a large temperature gradient not only in the radial direction, but also in the axial one.

The capsule containing a heat pipe is shown in Fig. 2. The evaporator of the heat pipe is positioned in the JMTR core, and its condenser is located out of the top of the core. A large part of heat generated in the capsule can be transferred upward through the heat pipe axis to the coolant above the core, and the rest through the capsule wall to the outer surface of the container. In this way the heat pipe removes a great amount of heat from the capsule, permitting the temperature distribution of the capsule to be more uniform.

For the design of heat pipes, the most important thing is to predict their thermal performances by calculation and experiment. Therefore, the heat pipe theory and various mathematic models have been set up in previous. Many computer programs have been developed for the heat pipe design. One of them is the Steady-state Heat Pipe Analysis Program, HTPIPE, written in a structured FORTRAN 77 by the scientists[1] of Los Alamos National Laboratory which has been in the lead on heat pipe research.

All the heat pipes used for irradiation capsules in reactors are of the vertical gravity-assisted heat pipe whose evaporator is vertically downwards installed. In this case, two of the most common structures are the axially grooved and the wickless heat pipes that operate mainly relying on the gravity, instead of the capillary, to return the working fluid from its condenser to its evaporator. Both of them not only have great heat transfer capability, but also are very easy to be fabricated and quite reliable in operation. Using the computer program HTPIPE on the computer FACOM M-780, we calculated the pressure profiles, the temperature profiles and the heat transfer limits of the wickless heat pipes in various sizes and working conditions in order to estimate their heat transfer capability and analyse their thermal performances. The calculation for the entrainment limit of the axially grooved heat pipes at various vapor temperatures has been completed by using the formulas in the reference 3. All the results are given in the following sections.

2. Calculated Results

2.1 Power Limits of the Wickless Water Heat Pipe

The power limits of the wickless heat pipe with a smooth wall have been calculated by HTPIPE[1]. For the vertical gravity-assisted wickless heat pipes with working fluid of water, the computer code provides both the sonic and entrainment limits which are considered as the main controlling limits.

The calculated results of the entrainment limit are shown in Table 1 and Fig. 3 for the nine heat pipes, 100 cm long each (evaporator 50 cm, condenser 50 cm), the inner diameters in the range from 0.8 to 5.0 cm, working at an evaporator exit temperature in the range from 300 to 500 K, in which water heat pipes usually operate. The calculational sonic limits of these heat pipes are given in Table 2. At high temperature points, the data of the sonic limits are so large (over 1000 kW) that they are not needed to be presented.

The relationships between the entrainment limits and the geometric sizes of heat pipes are shown in Fig. 4. It indicates that the entrainment limits are going up in quadratic dependence with the increase in their inside diameters, or in other words, they are in proportion to the cross sectional area of the axial vapor passages in heat pipes.

The entrainment limit and the sonic limit for the heat pipes with different condenser lengths and tilt angles were also calculated. The results proved that both have no change with an increase of either condenser length from 40 to 100 cm, or the tilt angles from 0 to 90°, or with a simultaneous increase in both of them.

To investigate the heat transfer characteristics of a long wickless water heat pipe, the calculation of its power limits was carried out. Its geometric parameters are given as follows:

Evaporator Length: 75 cm
Adiabatic Length: 25 cm
Condenser Length: 200 cm
Inside Diameter : 1.0 cm
Tilt Angle : 90° (gravity-assisted)

The calculated results are listed in Table 3.

2.2 Power Limits of the Grooved Water Heat Pipe

In order to compare with wickless heat pipes, the power limits of the axially grooved heat pipe, the structure of which is depicted below, have been estimated with the formulas in reference 3, which are shown as follows:

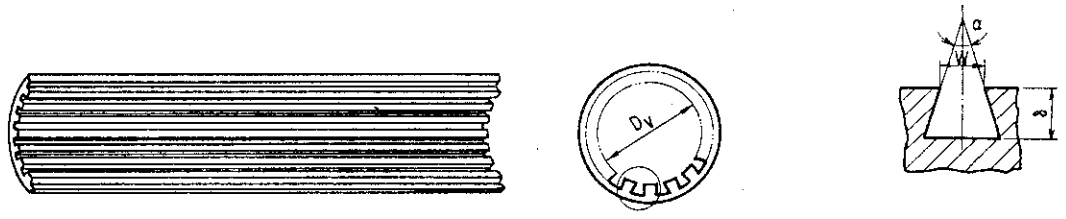

The structure of the Axial Trapezoid-grooved Heat Pipe

Entrainment limit is:

$$Q_{entra} = C_K^2 (D_v/w)^{1/2} A_v L [\rho_l^{1/4} + \rho_v^{1/4}]^{-2} [g\sigma(\rho_l - \rho_v)]^{1/4} \quad \cdots\cdots (1)$$

Where C_k is a coefficient relative to the Bond number, defined as:

$$C_K = 3.2^{1/2} \mathrm{th}(0.5 B_0^{1/4}) \quad \cdots\cdots (2)$$

Bond number: $B_0 = D_v [g(\rho_l - \rho_v)/\sigma]^{1/2}$ $\cdots\cdots (3)$

Sonic limit is expressed as:

$$Q_{sonic} = A_v L (P_{v,0}\ \rho_{v,0})^{1/2} (\gamma/[2(\gamma+1)])^{1/2} \quad \cdots\cdots (4)$$

Capillary limit is described as:

$$Q_{cap} = \frac{2\sigma/w - \rho_l g D_v \sin\beta + \rho_l g \ell \cos\beta}{[\mu_l/KA_w\rho_l L + (32\mu_v(1+\Phi)\phi_v/\rho_v L A_v D_v^2)]\ell_{eff}} \quad \cdots\cdots (5)$$

where: $$\Phi = \frac{D_v}{4\delta(1-0.314\ w/\delta)}$$

$$\phi_v = \begin{cases} 1 & R_e < 2000 \\ 0.00494 R_e^{5/4} & R_e \geq 2000 \end{cases}$$

Reynolds number:

$$R_e = \frac{4Q_{cap}}{\pi D_v\ \mu_v L}$$

Coefficient:

$$K = \frac{D_h^2}{2(fR_e)}$$

$$D_h = \frac{4\delta w}{w + 2\delta}$$

The total cross sectional area of the axial grooves is:

$$A_w = n(w\delta + \delta^2 tg\frac{\alpha}{2})$$

Effective length of the heat pipe is:

$$\ell_{eff} = \ell_a + (\ell_e + \ell_c)/2$$

The other symbols in the equations above are as follows:

ρ_l, ρ_v : the density of saturated water and vapor (kg/m^3)

σ : surface tension of water (N/m)

L : latent heat (J/kg)

γ : specific heat ratio, = C_P/C_V, (γ=1.33 for water vapor)

$P_{v,o}$: the vapor pressure at the end of the heat pipe evaporator (N/m^2)

$\rho_{v,o}$: the vapor density at the end of the heat pipe evaporator (kg/m^3)

μ_l, μ_v : the viscosity of water and vapor ($N.s/m^2$)

g : gravity acceleration (m/s^2)

D_v : the diameter of vapor passage (m)

A_v : the cross-sectional area of vapor passage (m^2)

ℓ : the total length of the heat pipe (m)

ℓ_e : evaporator length (m)

ℓ_a : adiabatic length (m)

ℓ_c : condenser length (m)

n : the number of axial grooves

w : groove width (m)

δ : groove depth (m)

α : the angle of the trapezoid groove (see the construction above)

β : the angle between the vertical line and the axis of heat pipe (β=0 for the vertical gravity-assisted heat pipe)

$f.R_e$: a coefficient relative to w/δ (see Fig. 1.11 in reference 3. when w/δ=1, $f.R_e$=14.4)

The characteristic data of water are listed in Table 4 and the geometric parameters of the grooved heat pipe are given as follows:

ℓ	ℓ_e	ℓ_a	ℓ_c	n	w	δ	α	β
1.0m	0.5m	0	0.5m	18	0.001m	0.001m	60°	0

The calculated results of the power limits for the grooved heat pipe are shown in Table 5.

From the results in Table 5, it is demonstrated that the entrainment limit (Q_{entrn}) is the lowest one among the power limits. The most important thing is how to increase its entrainment limit for this type of heat pipes. According to the equation (1), it will be effective to reduce the groove width w. Table 6 and Fig. 5 show the relationship between the entrainment and the groove size.

2.3 Pressure and Temperature Profiles for Vertical Gravity-Assisted Wickless Heat Pipes

Pressure and temperature profiles along the heat pipe length have been calculated by HTPIPE in terms of the two thermal boundary conditions: the input power and the sink temperature. The calculated results for the wickless heat pipe are shown in Fig. 6 through Fig. 14, and those for the long wickless heat pipe in Fig. 15 through Fig. 20.

All the input data for each calculated sample are presented in the figures. Some input data for the wickless heat pipe, such as the heat input rate, the sink temperature, the heat transfer coefficient (sink to pipe) and the thermal conductivity of pipe wall, originate from the values estimated by means of the experiments on heat pipes (see sample No. B in reference 9). For the long wickless heat pipe, the assumed input data were used because no experiments on this type have been done up to now.

3. Discussions

Being Different from the homogeneous wick heat pipe that is usually limited in heat transfer capability owing to the boiling limit or the capillary limit, as shown in Table 1, Table 2 and Fig. 3, the wickless heat pipe often has a lower entrainment limit because of a shear interaction between the counter-flowing liquid and vapor stream. The shear stress exerted on the liquid by the vapor prevents the condensate from returning to the evaporator, causing a dry-out of the heated surface in the evaporator. Before the occurrence of entrainment, waves are formed at the liquid-vapor interface. When the vapor velocity goes up to a critical value, which is defined as:

$$V_{crit} = (2\pi\sigma/\lambda\rho_v)^{0.5}$$

The calculated results of the power limits for the grooved heat pipe are shown in Table 5.

From the results in Table 5, it is demonstrated that the entrainment limit (Q_{entrn}) is the lowest one among the power limits. The most important thing is how to increase its entrainment limit for this type of heat pipes. According to the equation (1), it will be effective to reduce the groove width w. Table 6 and Fig. 5 show the relationship between the entrainment and the groove size.

2.3 Pressure and Temperature Profiles for Vertical Gravity-Assisted Wickless Heat Pipes

Pressure and temperature profiles along the heat pipe length have been calculated by HTPIPE in terms of the two thermal boundary conditions: the input power and the sink temperature. The calculated results for the wickless heat pipe are shown in Fig. 6 through Fig. 14, and those for the long wickless heat pipe in Fig. 15 through Fig. 20.

All the input data for each calculated sample are presented in the figures. Some input data for the wickless heat pipe, such as the heat input rate, the sink temperature, the heat transfer coefficient (sink to pipe) and the thermal conductivity of pipe wall, originate from the values estimated by means of the experiments on heat pipes (see sample No. B in reference 9). For the long wickless heat pipe, the assumed input data were used because no experiments on this type have been done up to now.

3. Discussions

Being Different from the homogeneous wick heat pipe that is usually limited in heat transfer capability owing to the boiling limit or the capillary limit, as shown in Table 1, Table 2 and Fig. 3, the wickless heat pipe often has a lower entrainment limit because of a shear interaction between the counter-flowing liquid and vapor stream. The shear stress exerted on the liquid by the vapor prevents the condensate from returning to the evaporator, causing a dry-out of the heated surface in the evaporator. Before the occurrence of entrainment, waves are formed at the liquid-vapor interface. When the vapor velocity goes up to a critical value, which is defined as:

$$V_{crit} = (2\pi\sigma/\lambda\rho_v)^{0.5}$$

the wavy liquid film will be torn to droplets. Then the droplets will be involved in the vapor flow and carried back to the condenser again. Finally, the heat pipe may be burnt out due to the shortage of water on the heated surface in the evaporator. The wavelength is determined by the geometry of the underlying surface.

According to heat pipe theory, the entrainment limit can be increased by three measures: enlarging the diameter of the vapor passage, making grooves on the pipe wall, and covering the pipe wall with a wick. The first measure is the most effective and easy to be practised. As shown in Fig. 4, the entrainment limit of the wickless heat pipe is sharply going up with an increase of its inside diameter. This is the best way if there is a space enough to load a large size heat pipe in an irradiation capsule. The second one is a preferable way for the small capsules. From Fig. 21, it is found that the entrainment limit of the grooved heat pipe is much higher than that of the wickless one, although both have the same inside diameter. In Fig. 5, the calculation results indicate that a higher entrainment limit can be obtained by reducing the groove width of the heat pipe. The third measure, however, is not so good as expected. The calculated power limits of a homogeneous wick heat pipe (only as a calculation example) are shown in Table 7 and Fig. 22. The results point out that the heat transfer capability of the homogeneous wick heat pipe is mainly limited by its low boiling limit in the high temperature range over 420 K. At a temperature of 480 K, its boiling limit (about 1.6 kW) is too low to remove out the high dense heat of an irradiation capsule in the reactor core. Furthermore, its thermal stability and reliability rely strongly on the manufacturing technique and the operation condition. It means that its actual power limits may be lower than the calculated results and be gradually reduced after a long operation because of the improper contact between the mesh wick and the pipe wall.

In addition, Nguyen, Chi and Groll ever studied the vertical gravity-assisted wickless heat pipe[3]. Their study indicated that the vertical wickless heat pipe had other two power limits: the dry-out limit and the boiling limit. When inadequate condensate returns along the pipe wall to the liquid puddle at the evaporator bottom under a high heat flux, the dry-out will occure even without the entrainment existence. Their experimental results proved the dry-out limit would rise up with the

increase of both the fluid inventory and the condenser length. But unfortunately, no ripe theory and accurate formula have yet been reported to predict the two power limits for this kind of heat pipe, so it is very necessary to further study the relationships between the thermal performance and the liquid inventory as well as the geometry of the vertical gravity-assisted heat pipe by some experiments.

The pressure and the temperature profile for each wickless heat pipe, as shown in Fig. 6 through Fig. 20, have the same tendency because the vapor and the liquid are always at the saturation state. So the temperature profile is completely based on the pressure distribution. Normally, as seen in Fig. 6 through Fig. 14, the vapor pressure within the evaporator and the adiabatic zone is gradually falling down with the acceleration of vapor, and then going up within the condenser zone with the deceleration of vapor under a greater radial Reynolds number, defined as:

$$Re_r = \frac{\rho_v \gamma_v v_v}{\mu_v}$$

where γ_v is the radius of the vapor passage and v_v is the radial velocity of vapor. Generally speaking, the pressure recovery in the condenser exists only when $|Re_r| \gg 1$. In this case, the inertial effect is much stronger than that of the viscousity.

From Fig. 15 to Fig. 20, however, we have found a different result in which no pressure recovery exists in a long wickless heat pipe. This is because there is a very low radial heat flux over the condenser due to its long size or large condensing surface. Under the low heat flux, the vapor flow is laminar with a little radial Reynolds number, $|Re_r| \ll 1$, and the viscous effect exceeds the inertial. In the case, the vapor pressure is continually dropped in the condenser to conquer the viscous friction resistance.

The existence of pressure drop is needed to provide a driving force for maintaining the movement of the vapor and fluid flow in a heat pipe. But it causes a temperature difference which is not desirable. For the water heat pipe, however, the temperature difference is so little (lower than 0.1°C) that is acceptable. Therefore, an temperature profile so uniform as to be acceptable can be obtained in a water heat pipe.

As shown in Fig. 23, there is a temperature difference (T_V-T_O) between the vapor and the outside surface of the wickless heat pipe. The difference depends completely on the thermal resistance from the vapor

to the outside surface. The distribution of the temperature difference on the evaporator surface differs from that on the condenser. According to the theoretical model of a vertical gravity-assisted wickless heat pipe shown in the figure below, the fluid film on the inside wall is not uniform in thickness. The film thickness increases along the pipe length

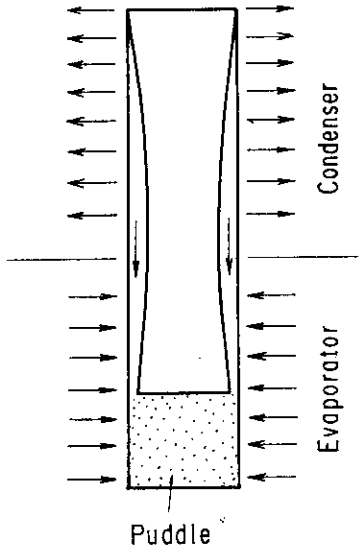

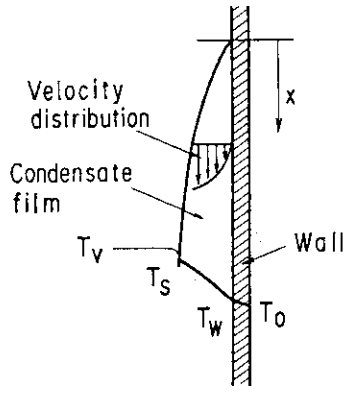

Film condensation on a vertical surface

The Theoretical Model of a Vertical Wickless Heat Pipe

from the condenser end to the evaporator exit where it reaches the maximum. Then the film gradually becomes thin until the liquid puddle because of the strong evaporation on the heated surface of the evaporator. In the evaporator region, the heat is transported to the liquid surface partly by conduction through the film and partly by natural convection. Evaporation is from the liquid surface. As the heat flux is high, the vapor bubbles form at nucleation sites. These bubbles transport a great amount of energy to the surface by latent heat of vaporation and also greatly improve convective heat transfer. So, as seen in Fig. 23, the temperature difference (T_O-T_V) over the evaporator region is not large and almost constant. In the condenser region, being different from that in the evaporator, the heat transfer from the liquid surface to the pipe wall is almost completely based on conduction through the liquid film under the film condensation condition which exists usually in heat pipes. In this case, a large temperature difference occurs because of the great thermal resistance of water, and increases continually with distance from the top of the condenser.

4. Conclusions

Based on the calculated results and the discussions above, the vertical gravity-assisted wickless heat pipe with a larger diameter can be used for the irradiation capsules in the reactor core. Not only has it a great capability of heat transportation and a high thermal stability, but also it is quite easily fabricated. In order to extend its entrainment limit, it is necessary to make some grooves on the inside surface of the pipe wall. Both the huge heat transfer ability and the excellent thermal stability can be obtained in the grooved heat pipe. The homogeneous mesh wicked heat pipe is preferable only at lower working temperatures (below 120°C), but it seems not to be good enough to operate at high temperatures (over 150°C) due to its low boiling limit.

All the discussions and conclusions above are made only based on the calculated results and the heat pipe theory. Considerably more work must be done to confirm the reliability of the theoritical calculations. Further study should be carried out to investigate the relationships between power limit and the working fluid inventory as well as the geometry of heat pipes by some experiments. Meanwhile, it is also extremely important to develop new kinds of high performance heat pipes for the irradiation capsules in the JMTR.

Acknowledgments

The authors are greatly indebted to Dr. Yoshiaki Futamura (Director of JMTR Project) for his support to the research. Mr. F. Nakayama (Deputy Manager of Irradiation Div. I), Mr. S. Suzuki (Irradiation Div.II), and Mr. T. Hoshiya provided much help and useful suggestions on the research. The authors are also very grateful to them.

References

(1) Keith A. Woloshun, Michael A. Merrigan, Elaine D. Best, "HTPIPE: A Steady-State Heat Pipe Analysis Program -- A User's Manual," November 1988, Los Alamos National Laboratory Document (U.S.A.), LA-11324-M.

(2) P.D. Dunn, D.A. Reay, "HEAT PIPES," Pergamon Press Ltd., Oxford, England, 1976.

4. Conclusions

Based on the calculated results and the discussions above, the vertical gravity-assisted wickless heat pipe with a larger diameter can be used for the irradiation capsules in the reactor core. Not only has it a great capability of heat transportation and a high thermal stability, but also it is quite easily fabricated. In order to extend its entrainment limit, it is necessary to make some grooves on the inside surface of the pipe wall. Both the huge heat transfer ability and the excellent thermal stability can be obtained in the grooved heat pipe. The homogeneous mesh wicked heat pipe is preferable only at lower working temperatures (below 120°C), but it seems not to be good enough to operate at high temperatures (over 150°C) due to its low boiling limit.

All the discussions and conclusions above are made only based on the calculated results and the heat pipe theory. Considerably more work must be done to confirm the reliability of the theoritical calculations. Further study should be carried out to investigate the relationships between power limit and the working fluid inventory as well as the geometry of heat pipes by some experiments. Meanwhile, it is also extremely important to develop new kinds of high performance heat pipes for the irradiation capsules in the JMTR.

Acknowledgments

The authors are greatly indebted to Dr. Yoshiaki Futamura (Director of JMTR Project) for his support to the research. Mr. F. Nakayama (Deputy Manager of Irradiation Div. I), Mr. S. Suzuki (Irradiation Div.II), and Mr. T. Hoshiya provided much help and useful suggestions on the research. The authors are also very grateful to them.

References

(1) Keith A. Woloshun, Michael A. Merrigan, Elaine D. Best, "HTPIPE: A Steady-State Heat Pipe Analysis Program -- A User's Manual," November 1988, Los Alamos National Laboratory Document (U.S.A.), LA-11324-M.

(2) P.D. Dunn, D.A. Reay, "HEAT PIPES," Pergamon Press Ltd., Oxford, England, 1976.

4. Conclusions

Based on the calculated results and the discussions above, the vertical gravity-assisted wickless heat pipe with a larger diameter can be used for the irradiation capsules in the reactor core. Not only has it a great capability of heat transportation and a high thermal stability, but also it is quite easily fabricated. In order to extend its entrainment limit, it is necessary to make some grooves on the inside surface of the pipe wall. Both the huge heat transfer ability and the excellent thermal stability can be obtained in the grooved heat pipe. The homogeneous mesh wicked heat pipe is preferable only at lower working temperatures (below 120°C), but it seems not to be good enough to operate at high temperatures (over 150°C) due to its low boiling limit.

All the discussions and conclusions above are made only based on the calculated results and the heat pipe theory. Considerably more work must be done to confirm the reliability of the theoritical calculations. Further study should be carried out to investigate the relationships between power limit and the working fluid inventory as well as the geometry of heat pipes by some experiments. Meanwhile, it is also extremely important to develop new kinds of high performance heat pipes for the irradiation capsules in the JMTR.

Acknowledgments

The authors are greatly indebted to Dr. Yoshiaki Futamura (Director of JMTR Project) for his support to the research. Mr. F. Nakayama (Deputy Manager of Irradiation Div. I), Mr. S. Suzuki (Irradiation Div.II), and Mr. T. Hoshiya provided much help and useful suggestions on the research. The authors are also very grateful to them.

References

(1) Keith A. Woloshun, Michael A. Merrigan, Elaine D. Best, "HTPIPE: A Steady-State Heat Pipe Analysis Program -- A User's Manual," November 1988, Los Alamos National Laboratory Document (U.S.A.), LA-11324-M.

(2) P.D. Dunn, D.A. Reay, "HEAT PIPES," Pergamon Press Ltd., Oxford, England, 1976.

(3) Ma Tongze, Hou Zhenqi, Wu Wenxi, "HEAT PIPES," Science Press, Beijing, China, 1983.

(4) Walter B. Olstad, "Heat Transfer, Thermal Control, and Heat Pipes," Published by the American Institute of Aeronauties and Astronauties, New York, 1980.

(5) J.E. Deverall, E.S. Keddy, J.E. Kemme and J.R. Phillips, "Gravity-Assist Heat Pipes for Thermal Control Systems," June 1975, Los Alamos Scientific Laboratory of the University of California, Report LA-5989-MS.

(6) Joseph E. Kemme, John E. Devera, Edward S. Keddy, "Performance of Gravity-Assist Heat Pipes with Screen-Wick Structures," Los Alamos Scientific Laboratory of the University of California, July 1974, LA-UR-74-212.

(7) S. Levy, "Prediction of Annular Liquid-Gas Flow with Entrainment -- Cocurrent Vertical Pipe Flow with Gravity," Electric Power Research Institute Document, EPRI NP-1521, September 1980.

(8) C.A. Busse, J.E. Kemme, "Dry-Out Phenomena in Gravity-Assist Heat Pipes with Capillary Flow," Int. J. Heat Mass Transfer, Vol. 23, pp. 643-654, Pergamon Press Ltd., Great Britain, 1980.

(9) Experiment Report on Stainless Steel Heat Pipes with Water as Working Fluid, JAERI Document FHP-88-190, Japan, August, 1988.

(10) Performance Production for Experimental Heat Pipes, JAERI Document FHP-88-139, Japan, April, 1988.

Table 1 Entrainment Limits for Wickless Heat Pipes

Temperature (K)	Q_{entrn}, (W)								
	Inside Diameter, D_i (cm)								
	0.8	1.0	1.6	2.0	2.6	3.2	4.0	4.4	5.0
300	185	299	799	1265	2161	3294	5173	6269	8112
320	290	467	1242	1963	3350	5102	8007	9703	12552
340	425	682	1808	2854	4865	7406	11619	14078	18209
360	588	940	2485	3920	6678	10163	15938	19310	24973
380	768	1233	3252	5126	8730	13282	20827	25231	32627
400	961	1544	4078	6428	10942	16646	26097	31614	40880
420	1159	1863	4939	7772	13228	20120	31541	38208	49403
440	1354	2178	5779	9106	15497	23569	36945	44754	57866
460	1538	2477	6579	10382	17662	26860	42104	51002	65943
480	1703	2746	7305	11531	19647	29860	42104	51002	65943
500	1841	2973	7920	12508	21318	32418	50816	61556	79590

Table 2 Sonic Limits of Wickless Heat Pipes

Temperature (K)	Q_{sonic}, (kW)								
	Inside Diameter, D_i (cm)								
	0.8	1.0	1.6	2.0	2.6	3.2	4.0	4.4	5.0
300	1.0	1.6	4.2	6.7	11.4	17.3	27.3	33.1	42.8
320	2.8	4.5	12.0	19.0	32.3	49.3	77.3	93.7	121.2
340	7.0	11.2	29.6	46.8	79.7	121.4	190.4	230.7	298.4
360	15.4	24.6	65.0	102.5	174.6	265.7	410.7	504.8	652.9
380	30.4	48.9	128.8	203.1	345.9	526.2	825.1	999.6	---
400	55.3	88.9	234.9	370.1	630.2	958.6	---	---	---
420	93.8	150.8	399.7	629.0	---	---	---	---	---
440	149.9	241.2	640.0	---	---	---	---	---	---
460	228.3	367.7	976.6	---	---	---	---	---	---
480	334.0	538.5	---	---	---	---	---	---	---
500	472.7	763.2	---	---	---	---	---	---	---

Table 3 Power Limits of the Long Wickless Heat Pipe

Temp.(K)	300	320	340	360	380	400	420	440	460	480	500
Q_{entrn}(W)	232	365	533	799	1180	1491	1814	2116	2390	2623	2800
Q_{sonic}(W)	849	2595	6810	15480	31645	58812	101446	164402	252818	371829	526052

Table 4 Characteristic Data of Water

T (^{o}C)	P.10^{5} (P_a)	L (kJ/kg)	σ .10^{3} (N/m)	ρ_v (kg/m^3)	ρ_l (kg/m^3)	μ_v.10^{5} (N.s/m^2)	μ_l.10^{5} (N.s/m^2)
20	0.023	2454	72.88	0.017	999	0.885	100.15
100	1.013	2251	58.91	0.597	959	1.210	27.90
200	15.551	1939	37.77	7.865	865	1.560	13.38

Table 5 Power Limits of the Axially Grooved Heat Pipe

T (^{o}C)	D_v = 10 (mm)		D_v = 20 (mm)		
	Q_{entrn} (kW)	Q_{sonic} (kW)	Q_{entrn} (kW)	Q_{sonic} (kW)	Q_{cap} (kW)
20	0.4	0.8	3.0	2.6	
100	1.7	3.3	13.3	92.9	
200	4.2	7.5	29.9	1135.3	2220.0

Table 6 The Entrainment Limits with Different Groove Sizes

(T = 200 °C P = 1.555×10^6 P_a)

groove width w (mm)	0.25	0.50	0.75	1.00	1.25	1.50
Q_{entrn} (kW) (D_v = 10 mm)	8.4	5.9	4.8	4.2	3.8	3.4
Q_{entrn} (kW) (D_v = 20 mm)	59.8	42.3	34.5	29.9	26.7	24.4

Table 7 Power Limits of the Homogeneous Wick Heat Pipe

Temperature (K)	Q_{sonic} (kW)	Q_{entrn} (kW)	Q_{cap} (kW)	Q_{boil} (kW)
300	6.78	17.79	14.99	41.63
320	19.18	28.53	24.81	23.44
340	47.20	42.59	38.05	31.25
360	103.20	59.78	54.66	20.11
380	204.24	79.57	74.25	13.34
400	371.85	101.13	96.17	8.53
420	631.43	123.49	119.63	5.47
440	---	145.58	143.80	3.58
460	---	166.31	167.88	2.39
480	---	184.53	190.99	1.63
500	---	198.99	212.15	1.14

Note: Input data of the heat pipe can be found in Fig.5

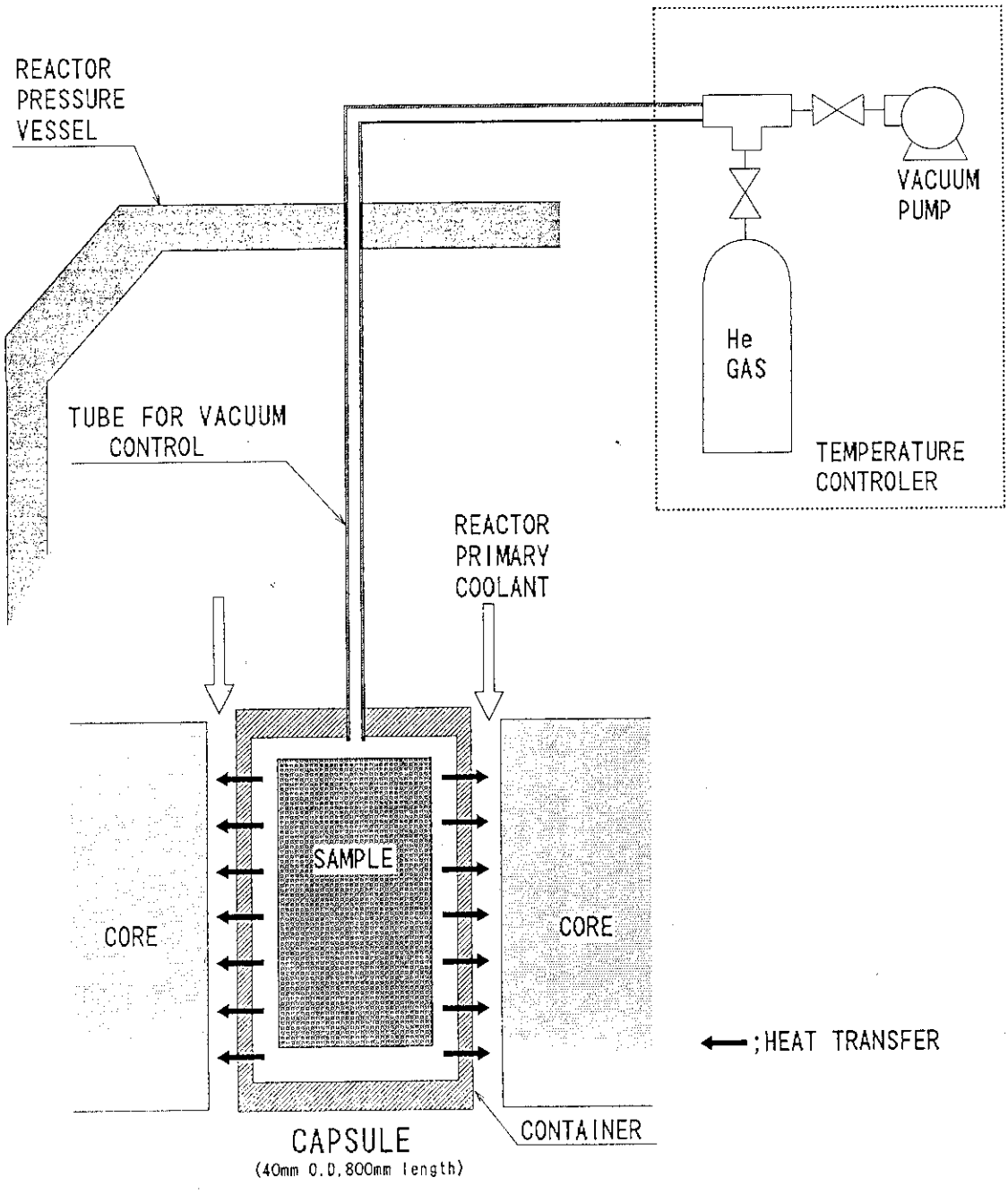

Fig. 1 Standard Capsule of the JMTR

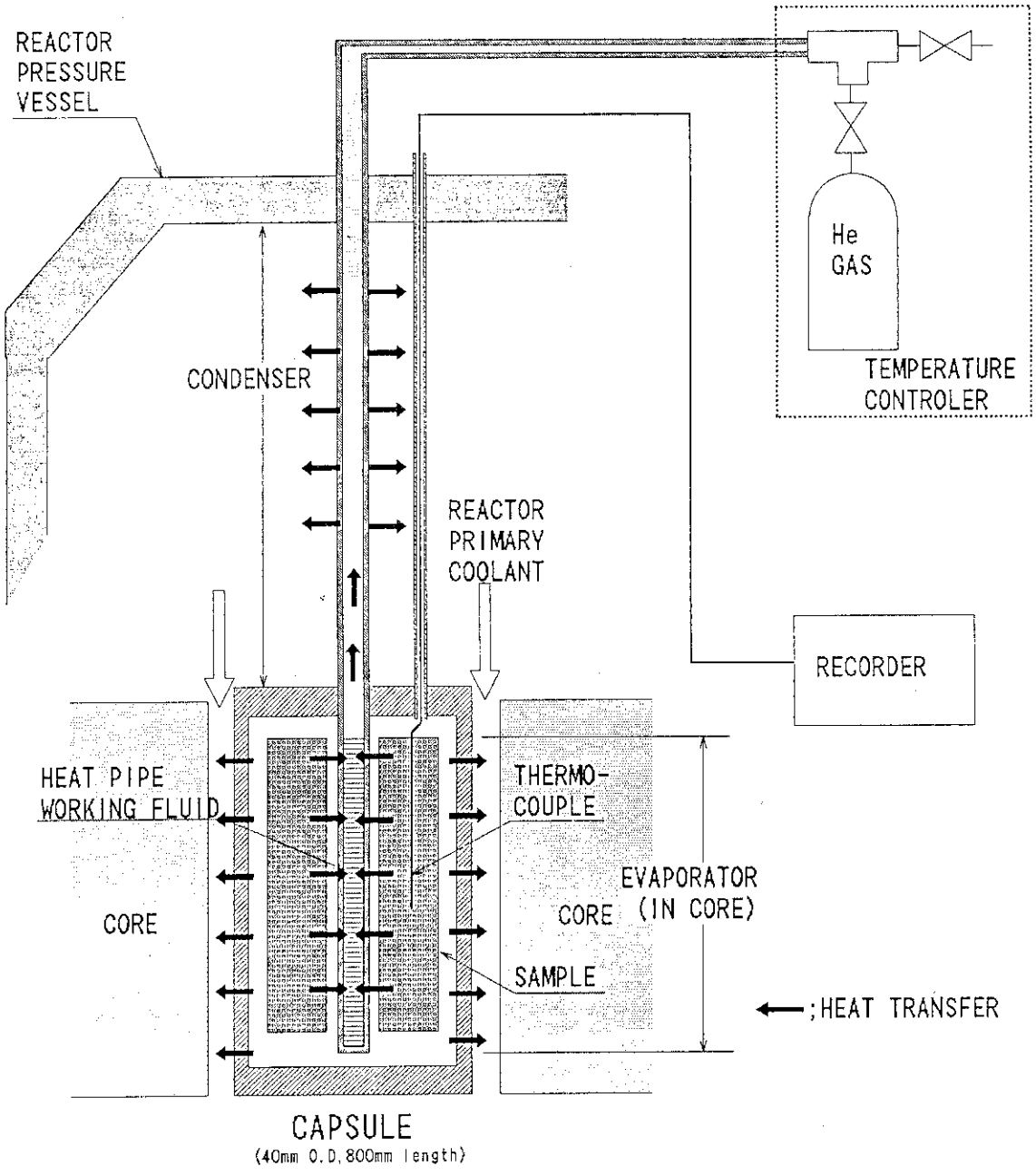

Fig. 2 Temperature Control System of the Capsule by Heat Pipe

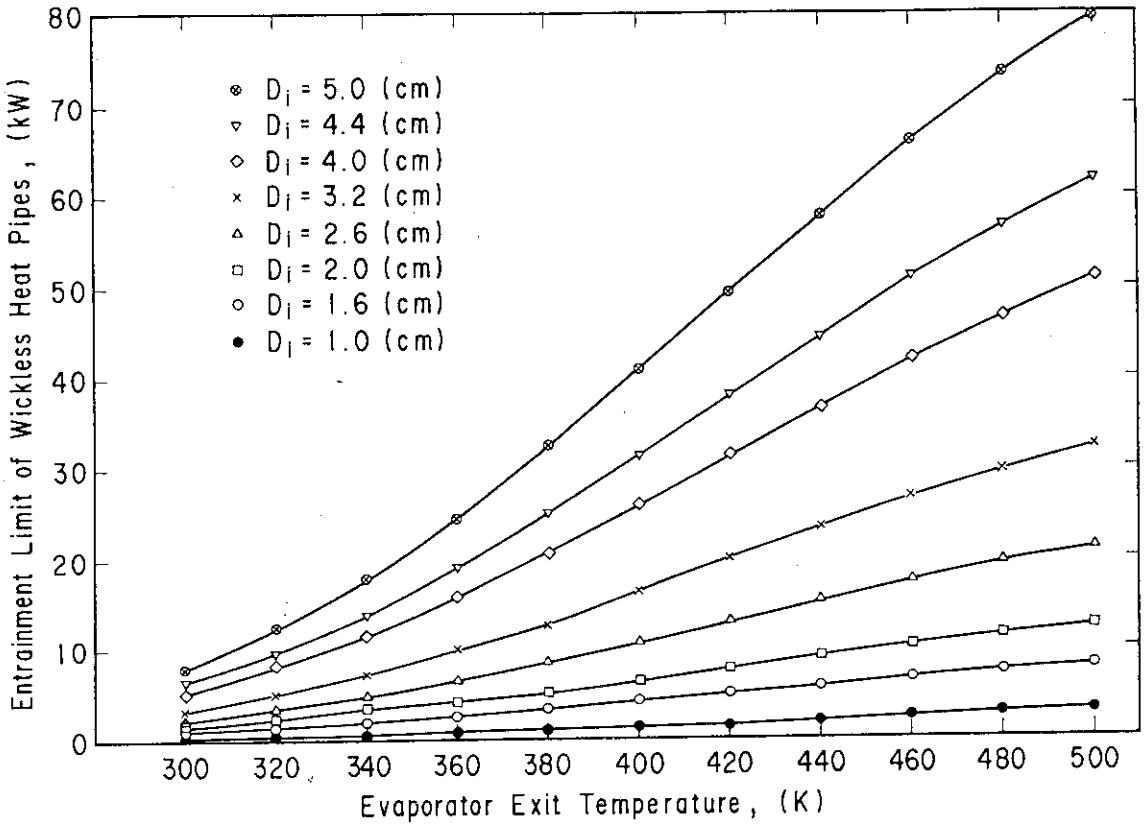

Fig. 3 Entrainment Limits of Wickless Heat Pipes with Different Inside Diameters

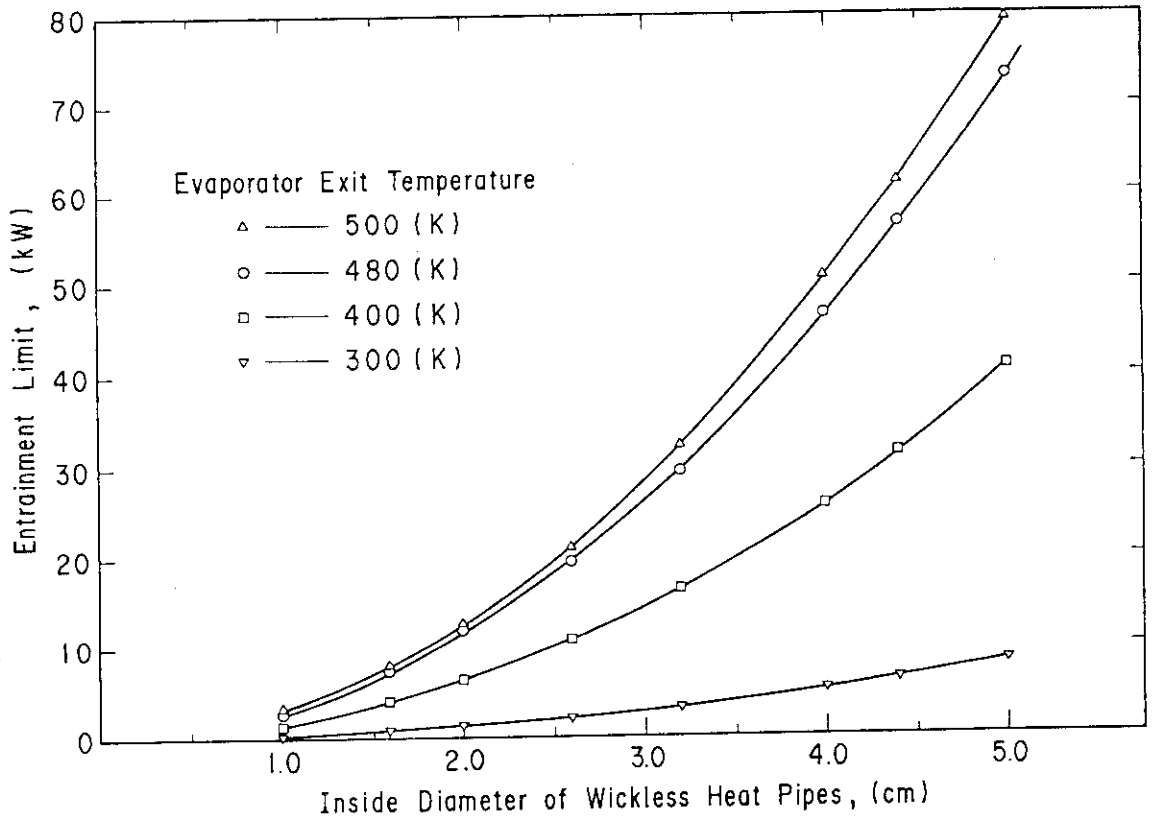

Fig. 4 Entrainment Limit Rising with the Increase of Inside Diameter

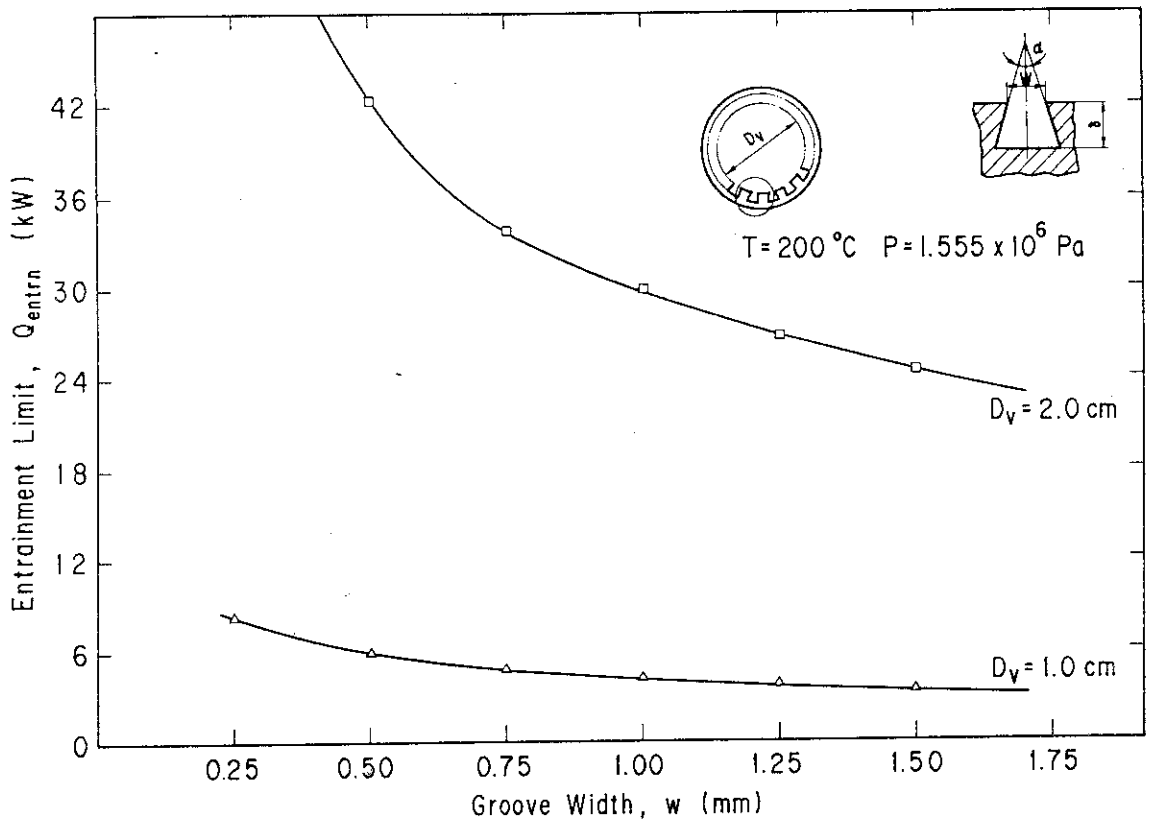

Fig. 5 The Relationship between the Entrainment Limit and the Groove Width

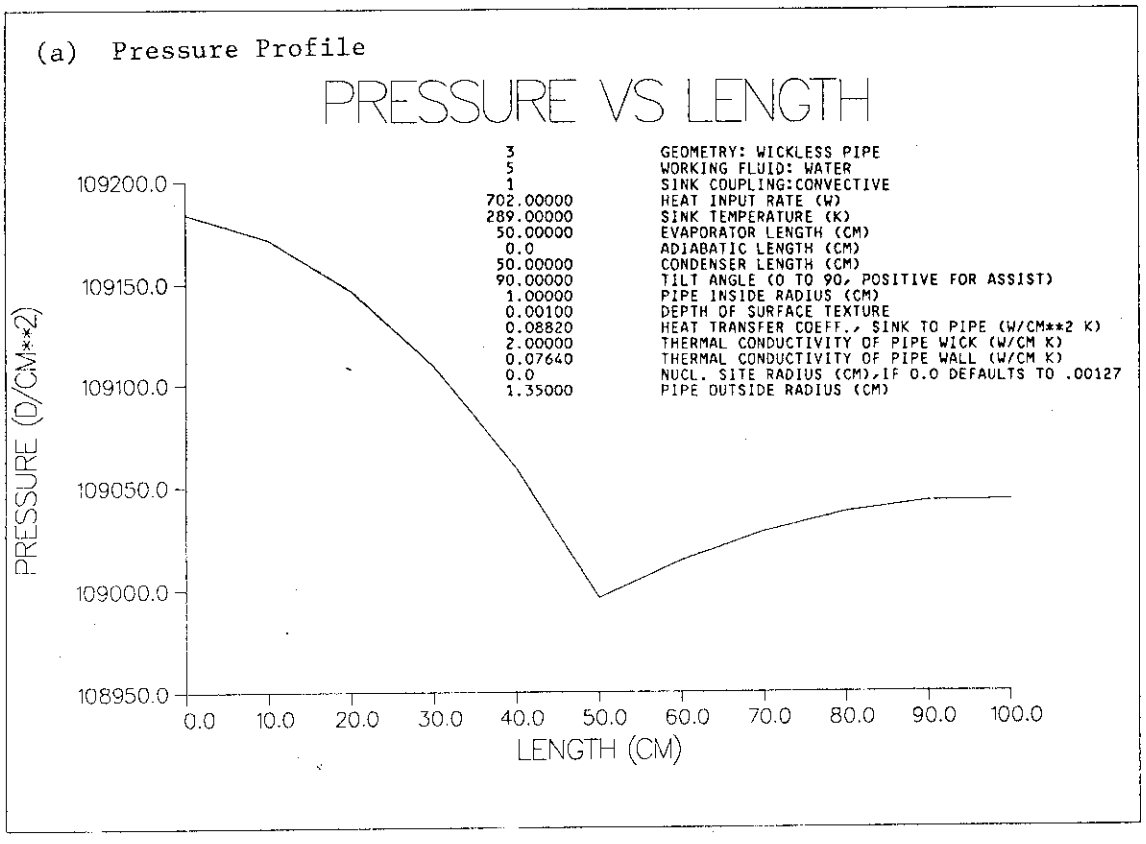

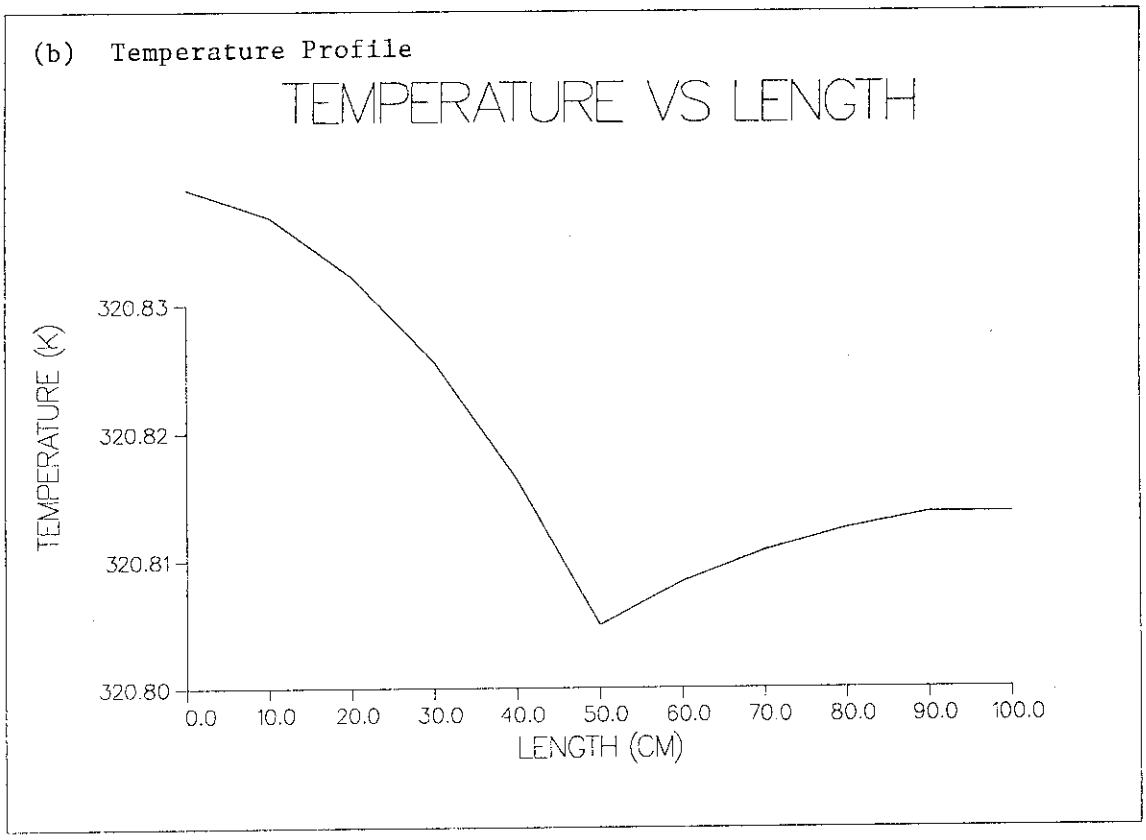

Fig. 6 Pressure and Temperature Profiles in the Wickless Heat Pipe (Input Power 702 W, Sink Temperature 289 K)

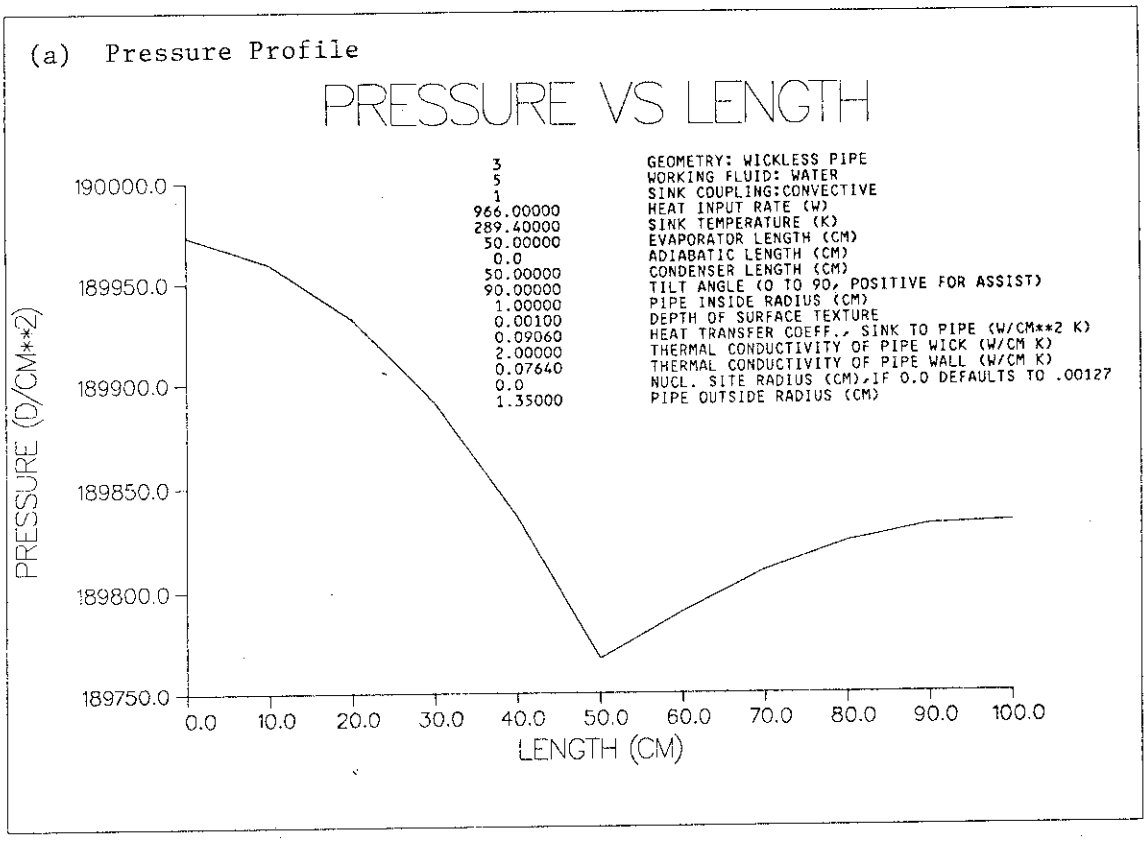

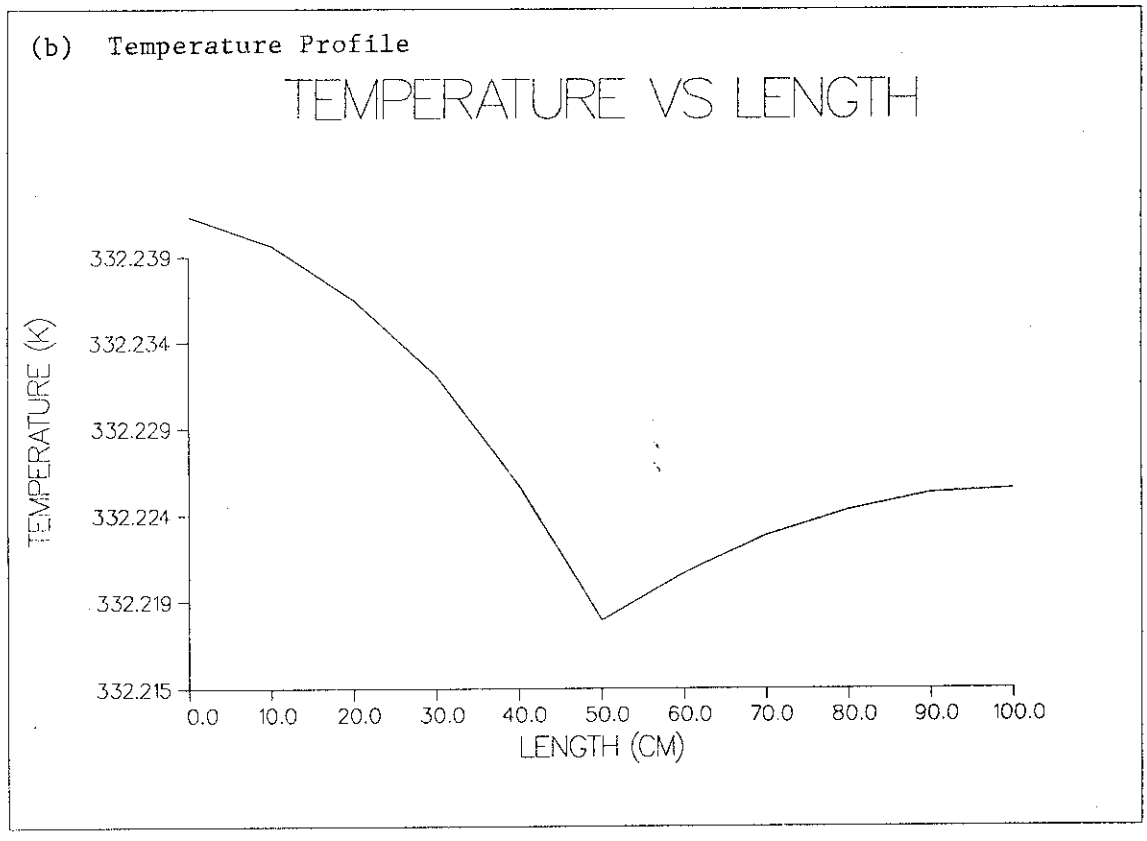

Fig. 7 Pressure and Temperature Profiles in the Wickless Heat Pipe (Input Power 966 W, Sink temperature 289.4 K)

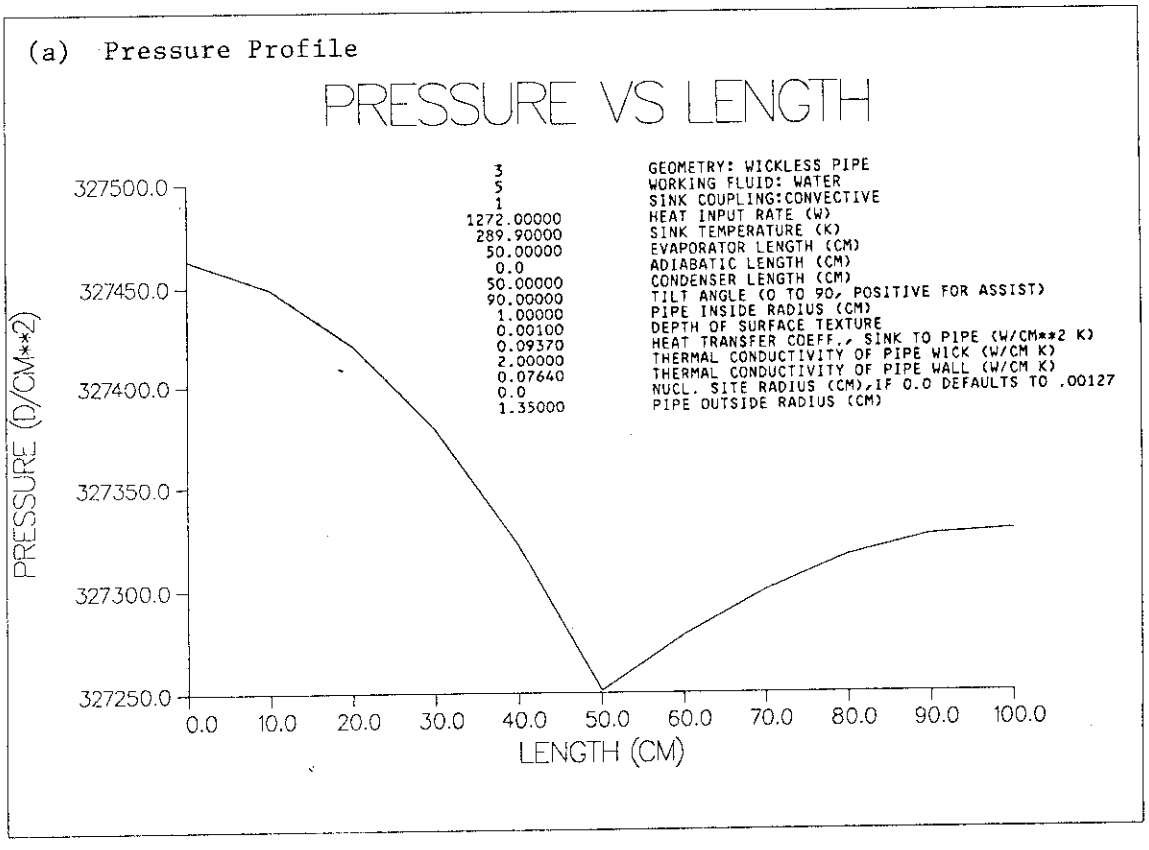

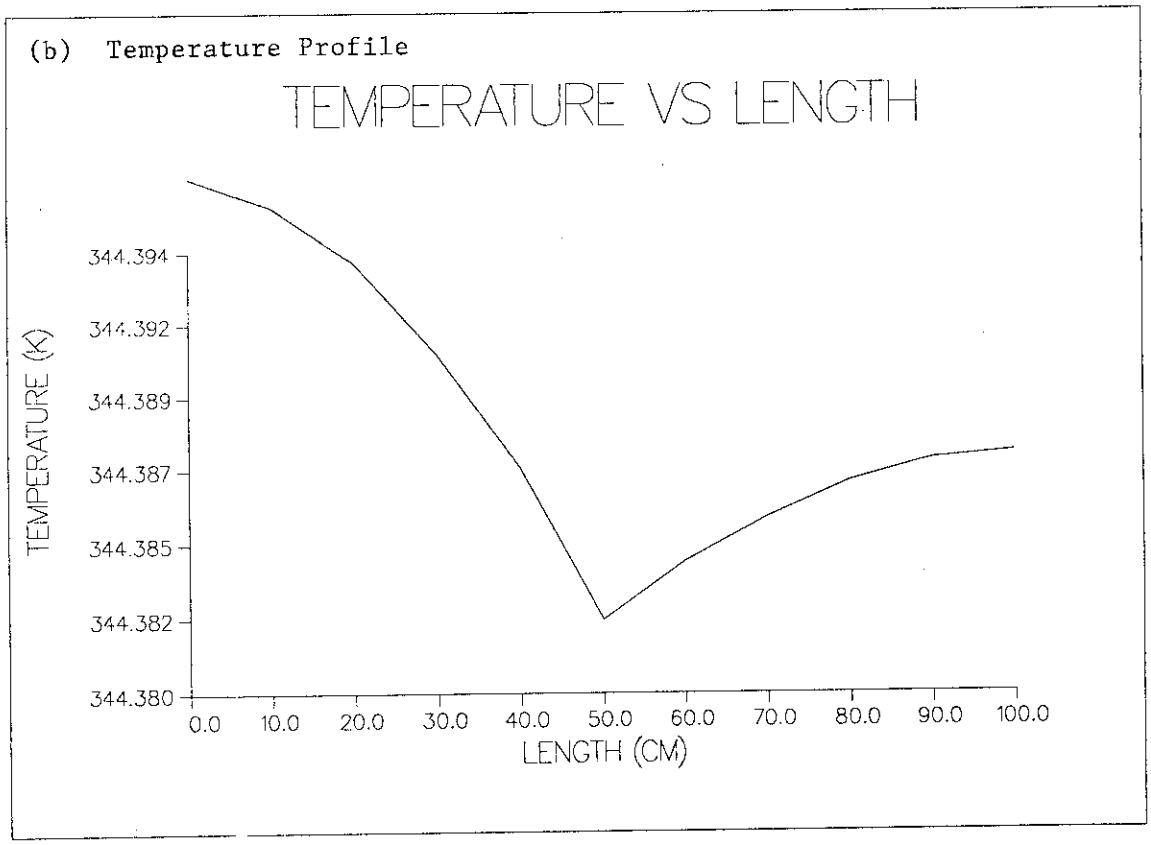

Fig. 8 Pressure and Temperature Profiles in the Wickless Heat Pipe (Input Power 1272 W, Sink Temperature 289.9 K)

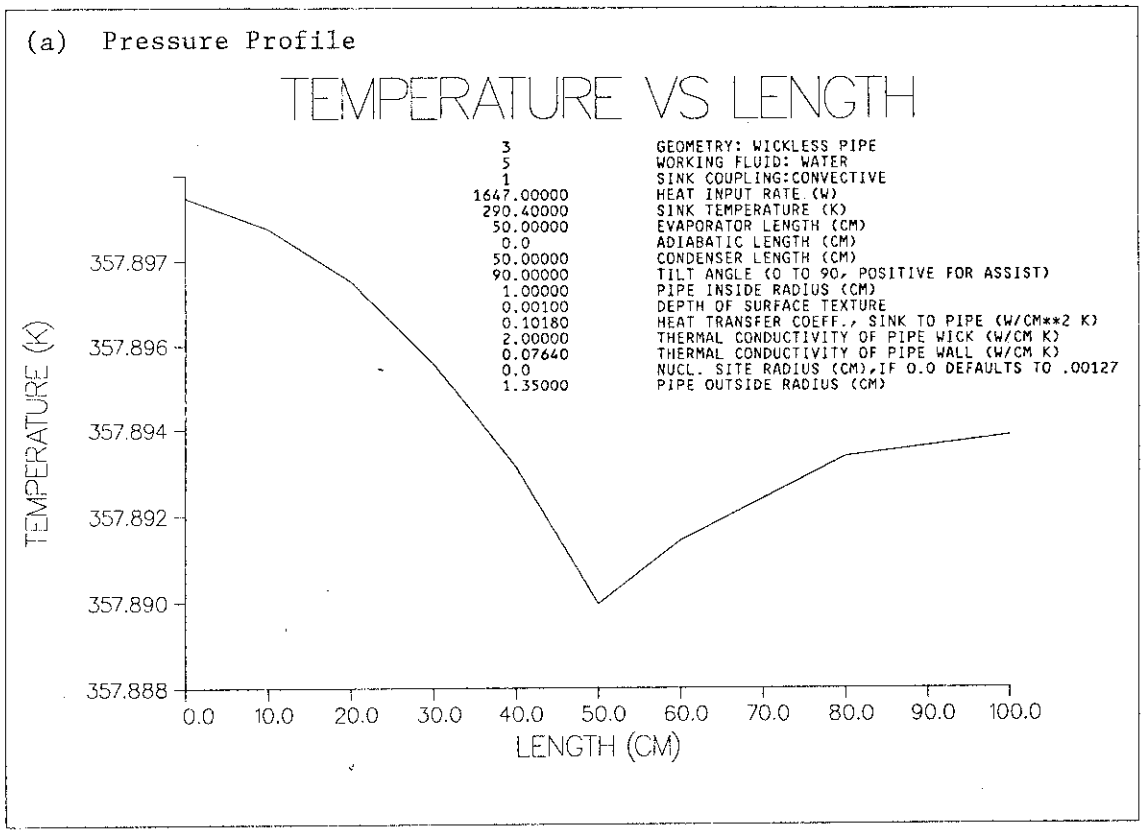

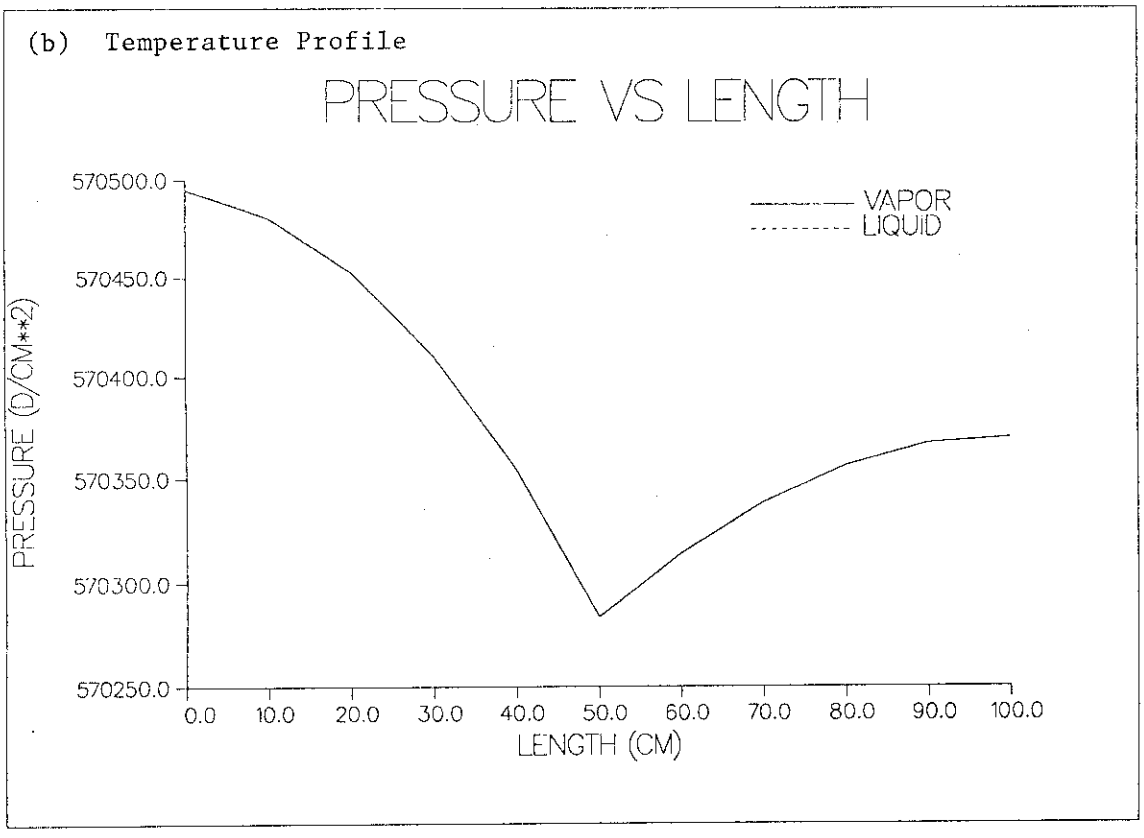

Fig. 9 Pressure and Temperature Profiles in the Wickless Heat Pipe (Input Power 1647 W, Sink Temperature 290.4 K)

(a) Pressure Profile

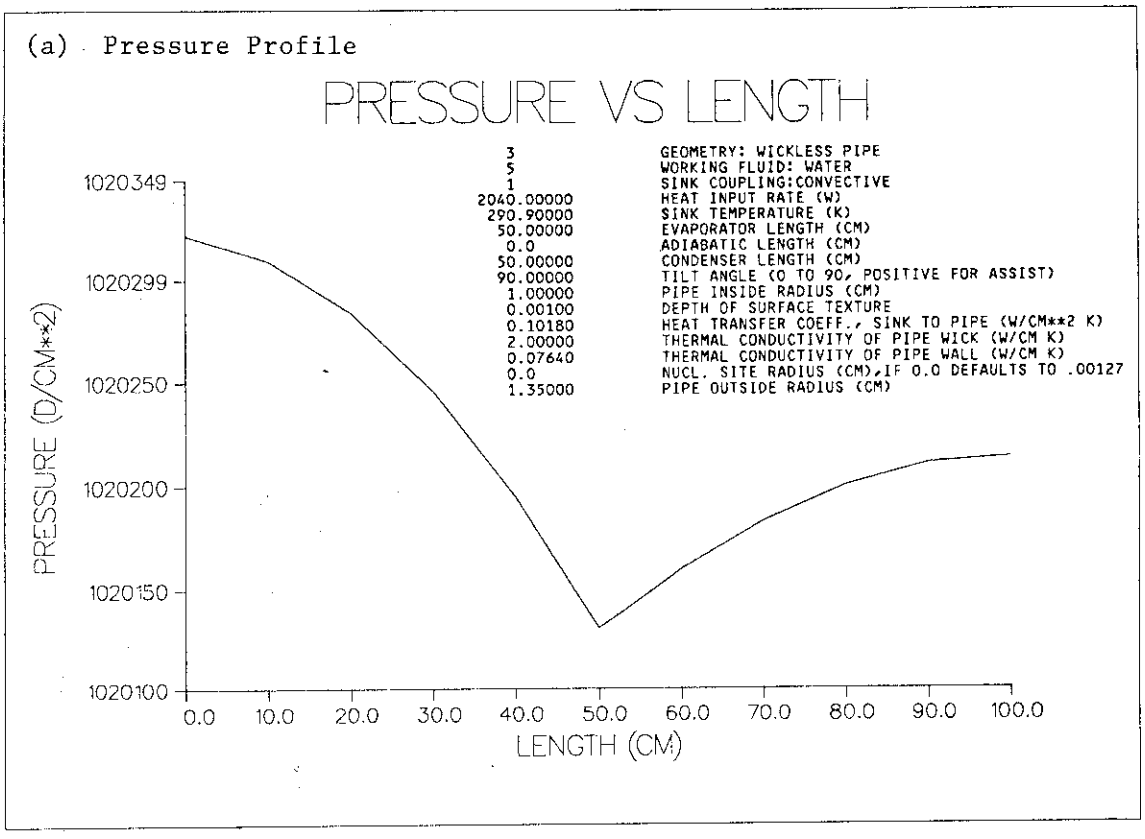

(b) Temperature Profile

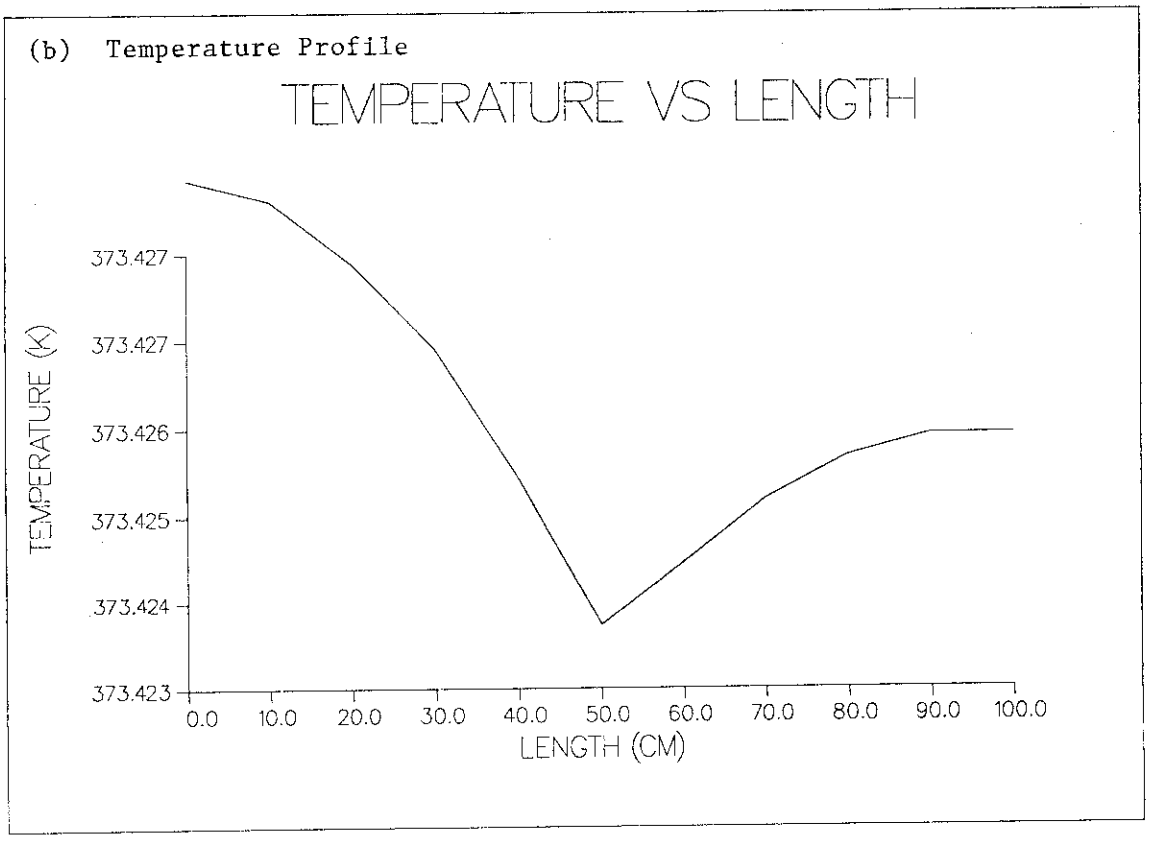

Fig. 10 Pressure and Temperature Profiles in the Wickless Heat Pipe (Input Power 2040 W, Sink Temperature 290.9 K)

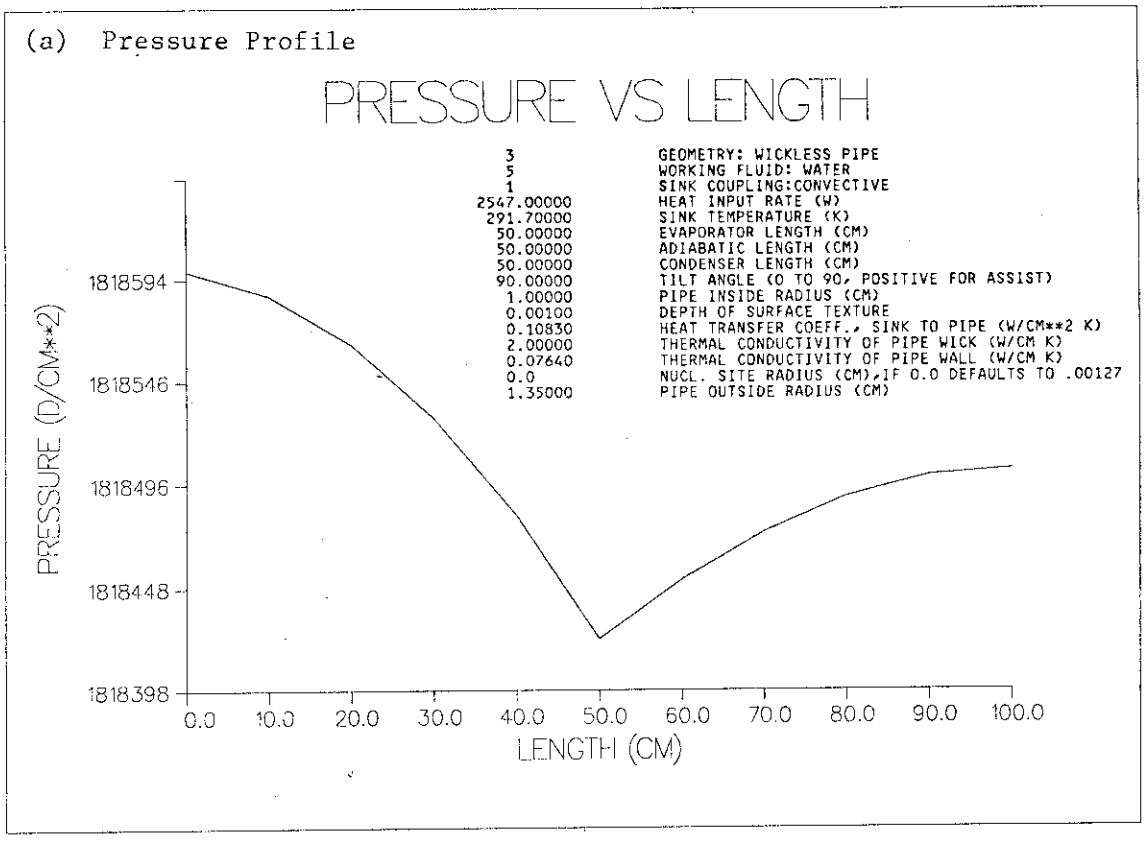

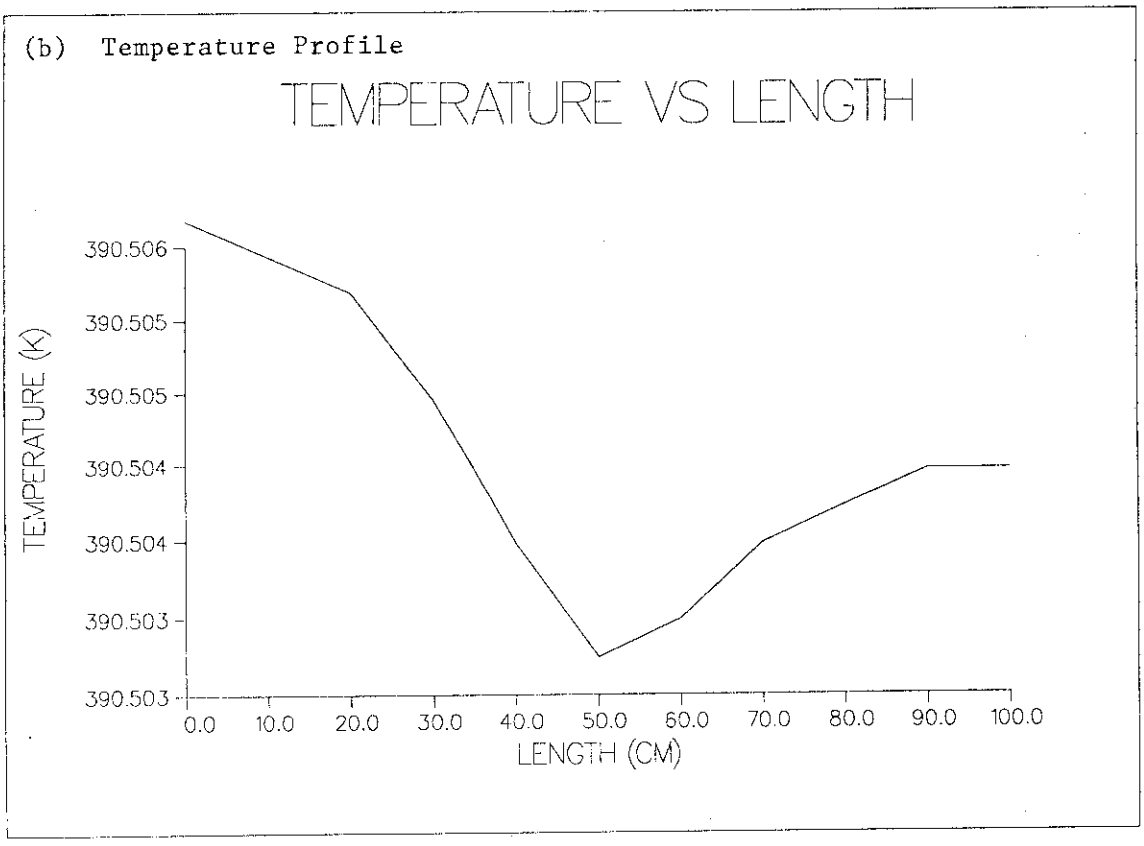

Fig. 11 Pressure and Temperature Profiles in the Wickless Heat Pipe (Input Power 2547 W, Sink Temperature 291.7 K)

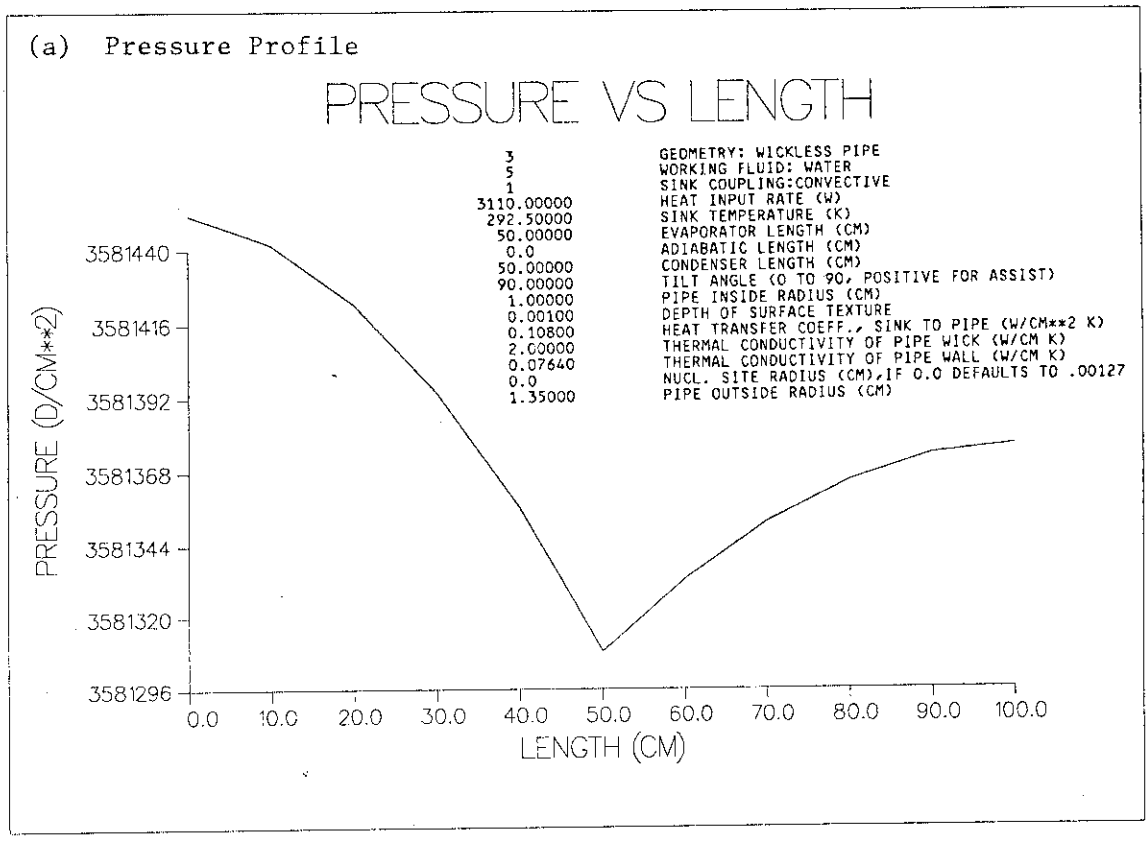

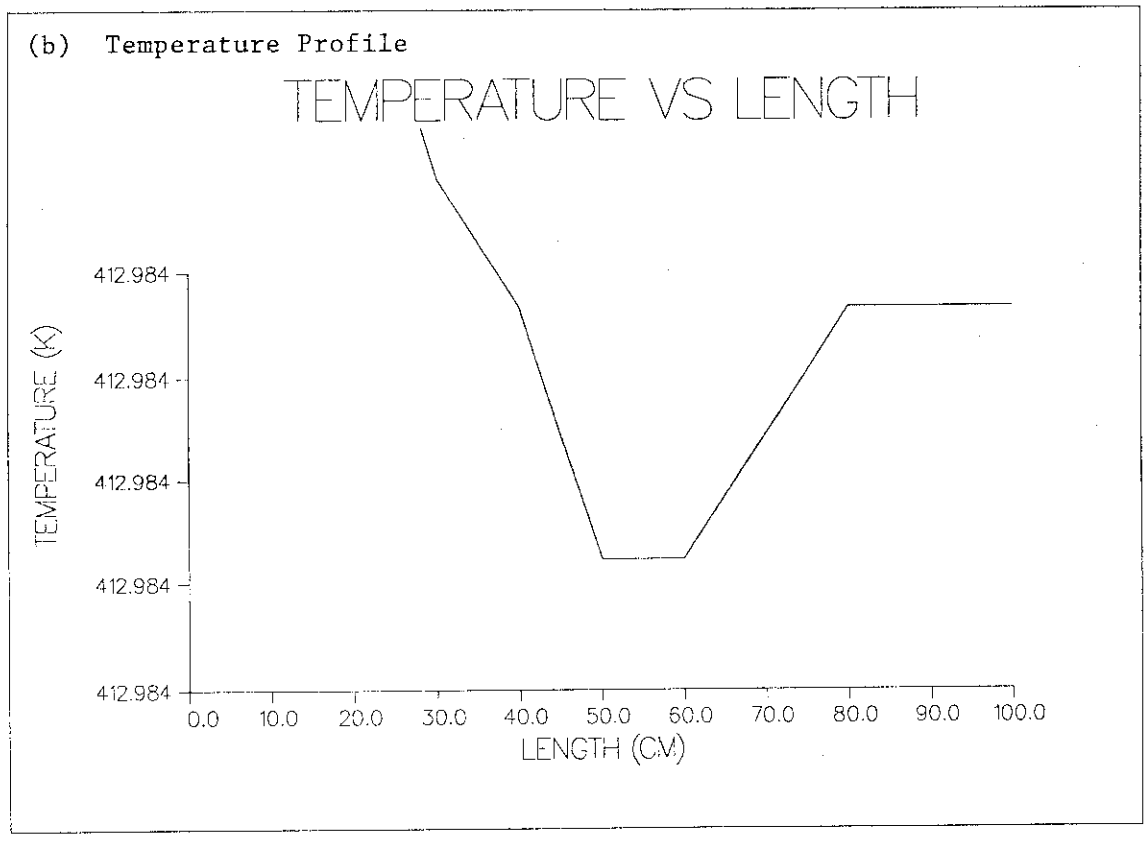

Fig. 12 Pressure and Temperature Profiles in the Wickless Heat Pipe (Input Power 3110 W, Sink Temperature 292.5 K)

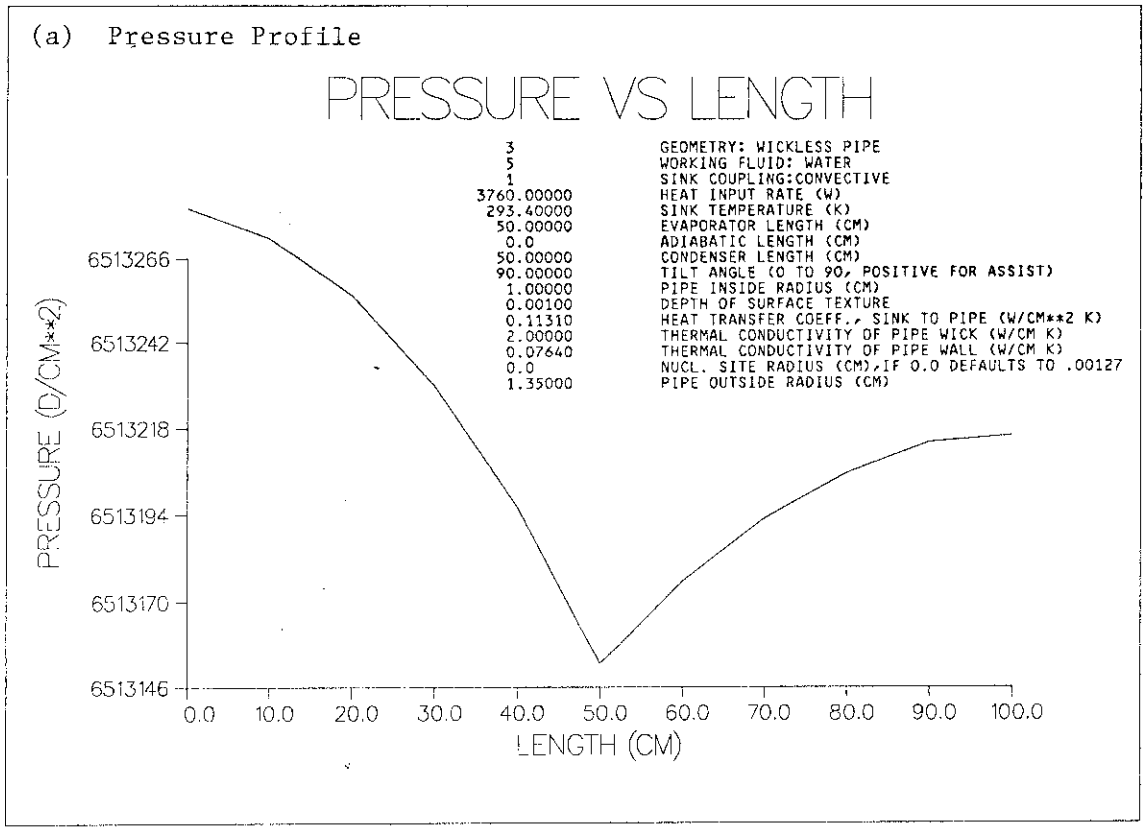

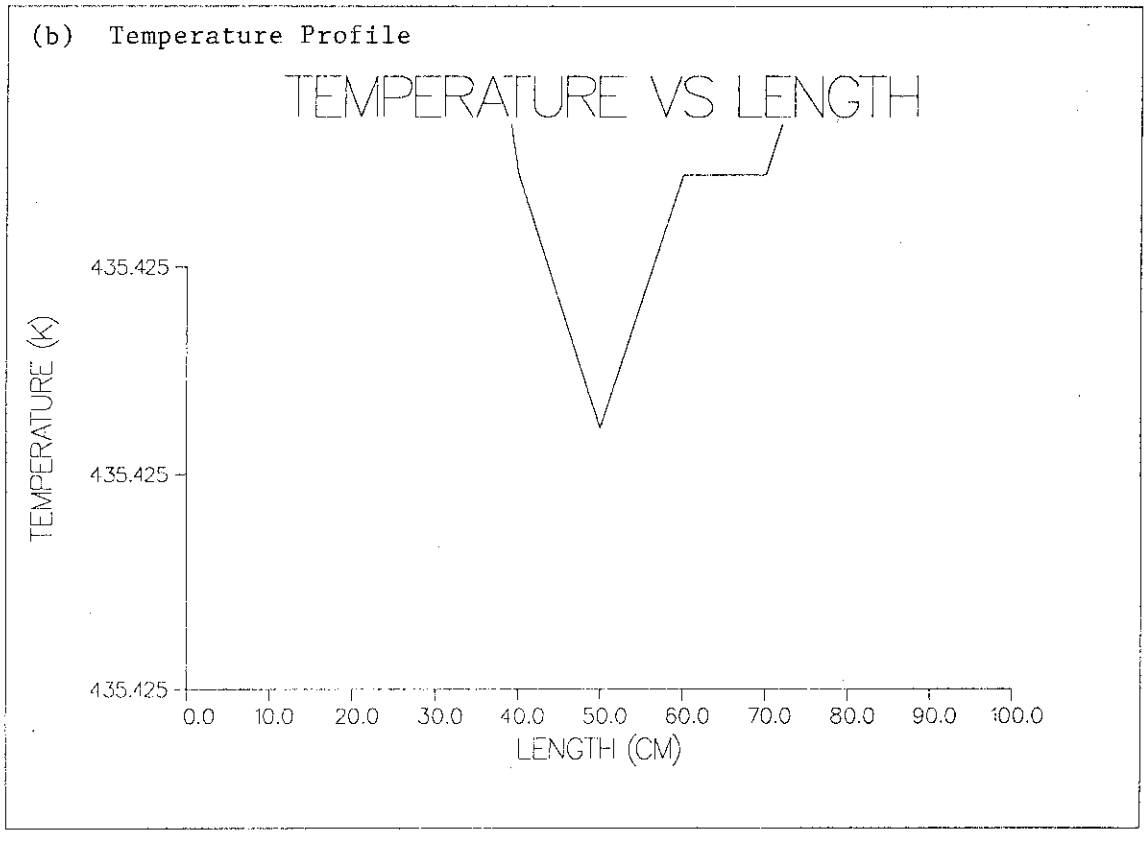

Fig. 13 Pressure and Temperature Profiles in the Wickless Heat Pipe (Input Power 3760 W, Sink Temperature 293.4 K)

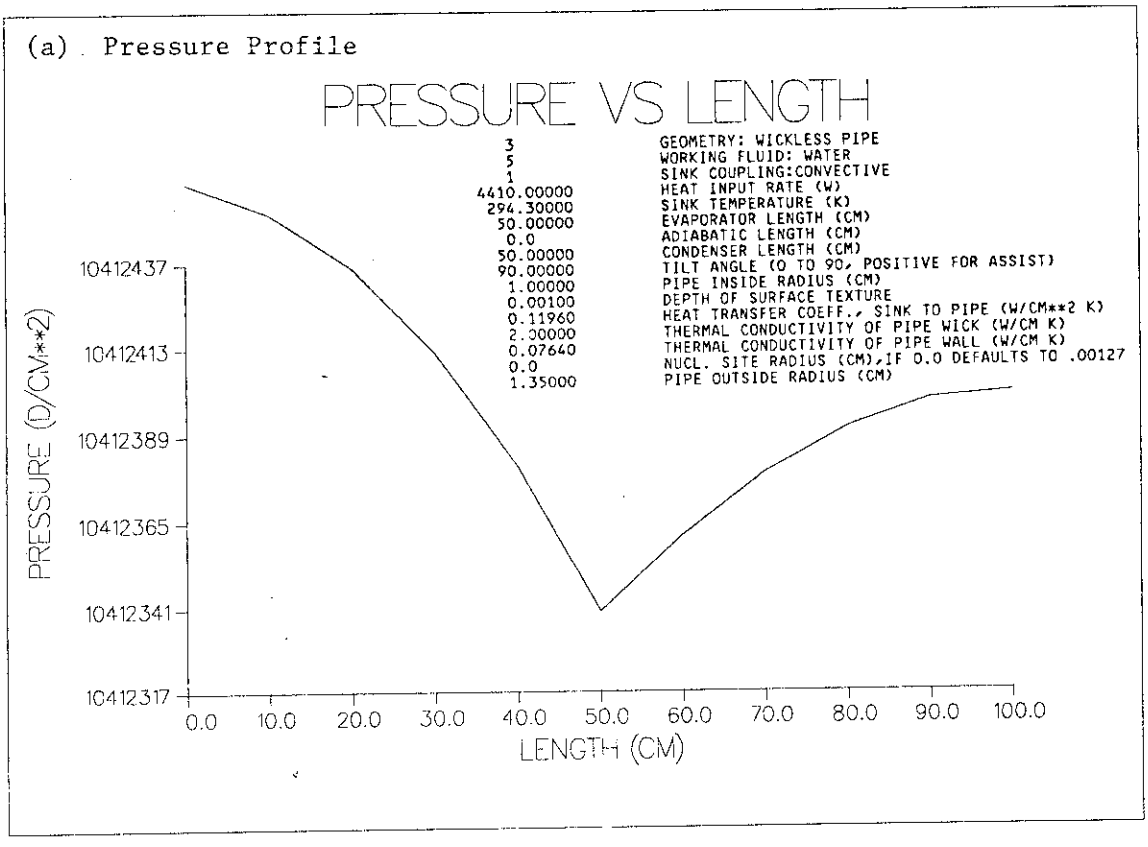

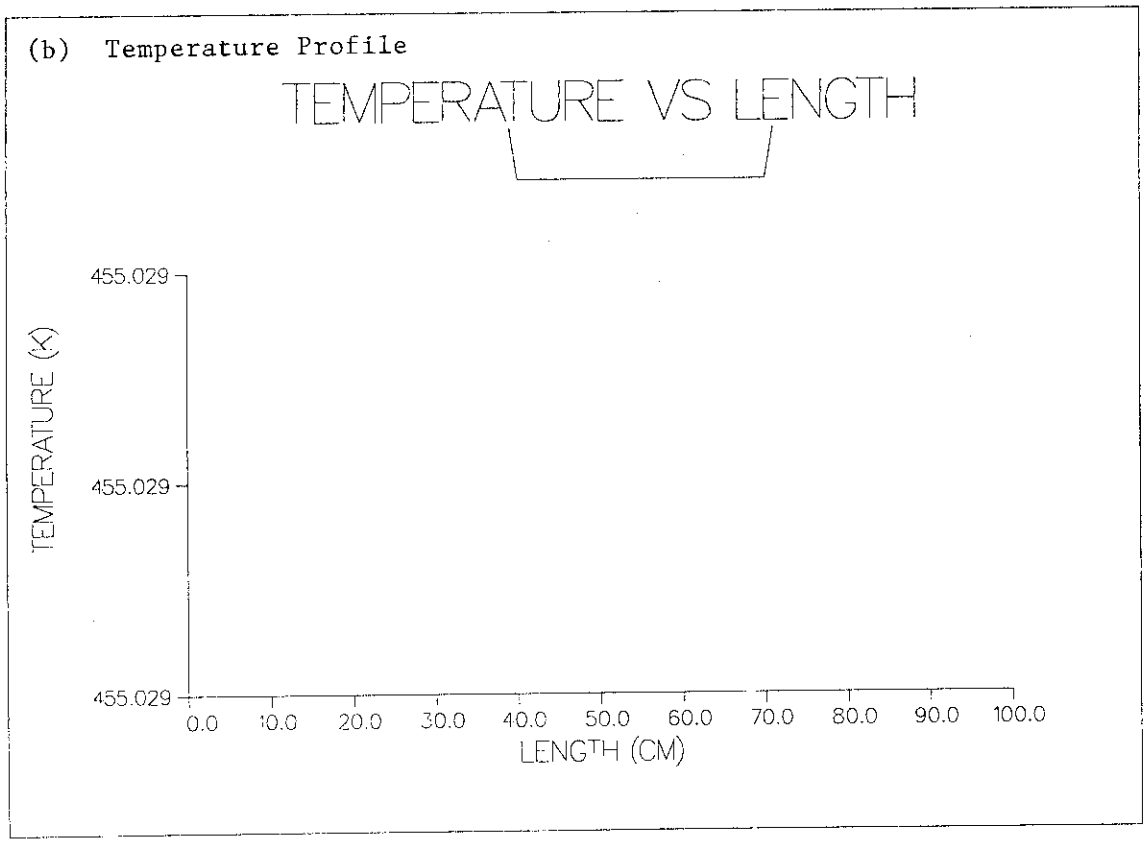

Fig. 14 Pressure and Temperature Profiles in the Wickless Heat Pipe (Input Power 4410 W, Sink Temperature 294.3 K)

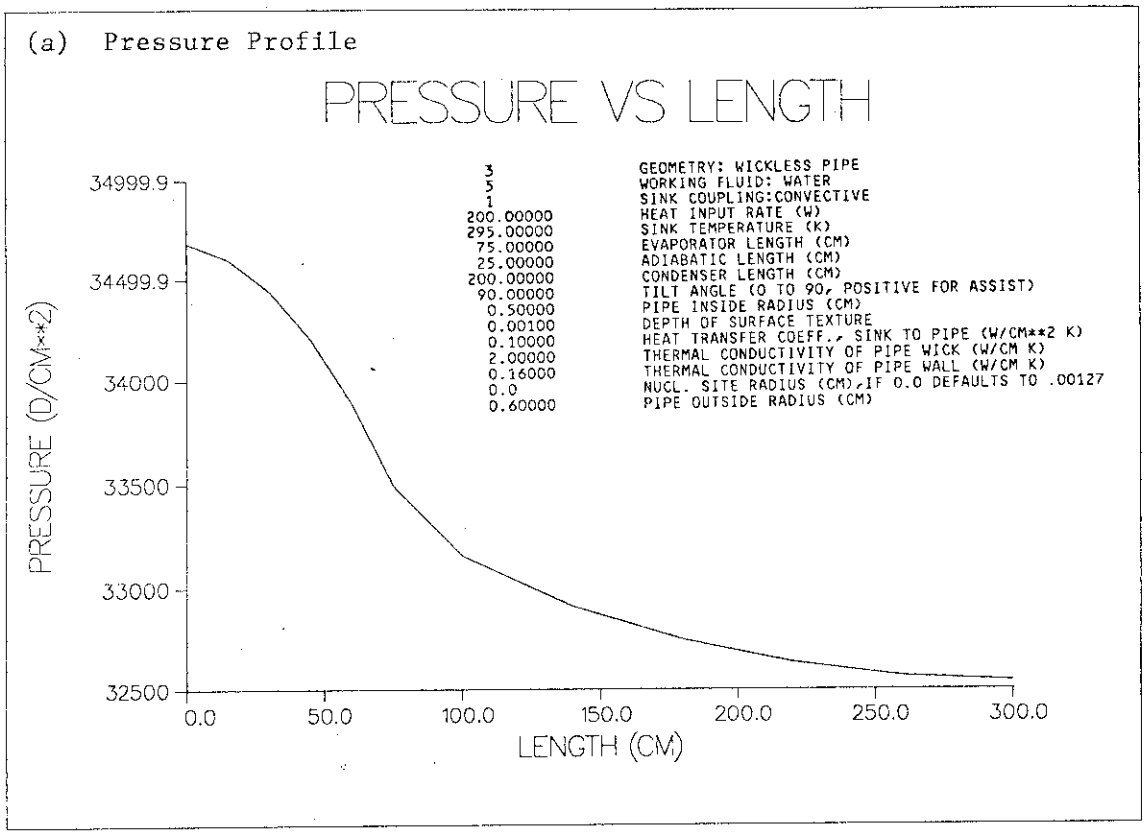

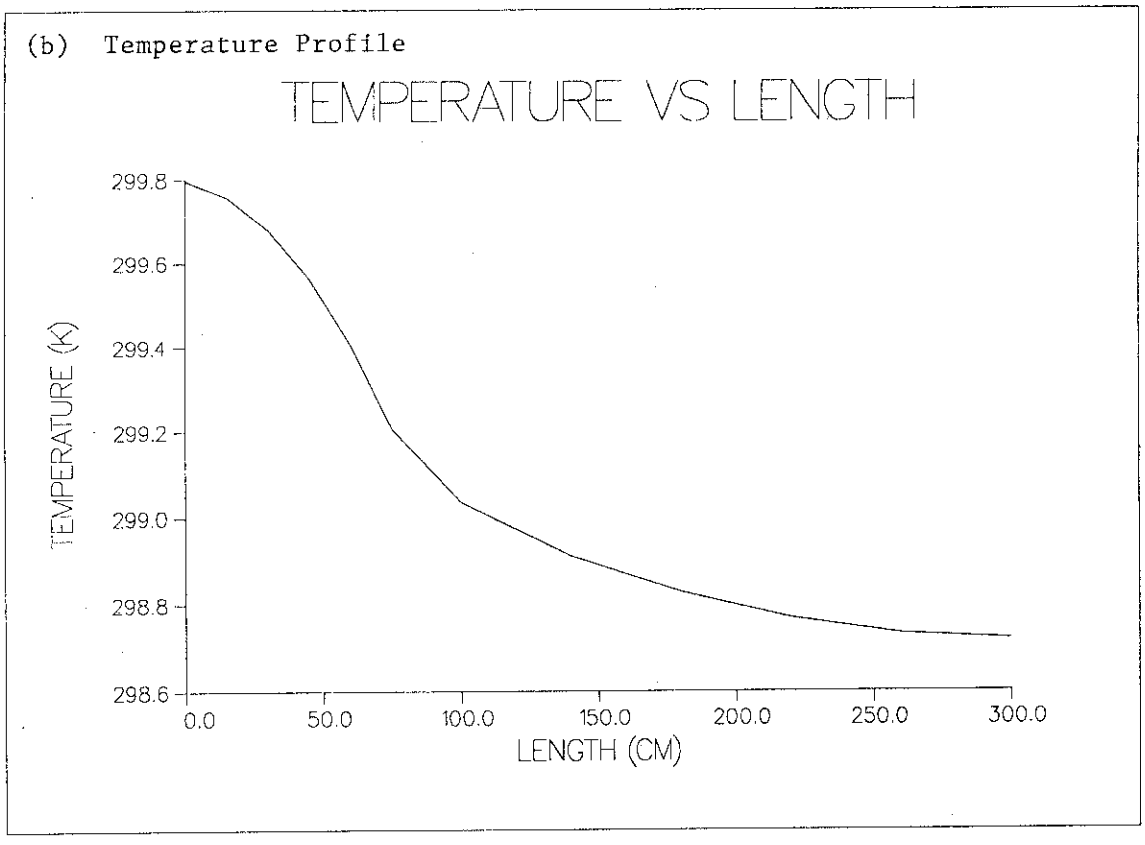

Fig. 15 Pressure and Temperature Profiles in the Long Wickless Heat Pipe (Input Power 200 W, Sink Temperature 295 K)

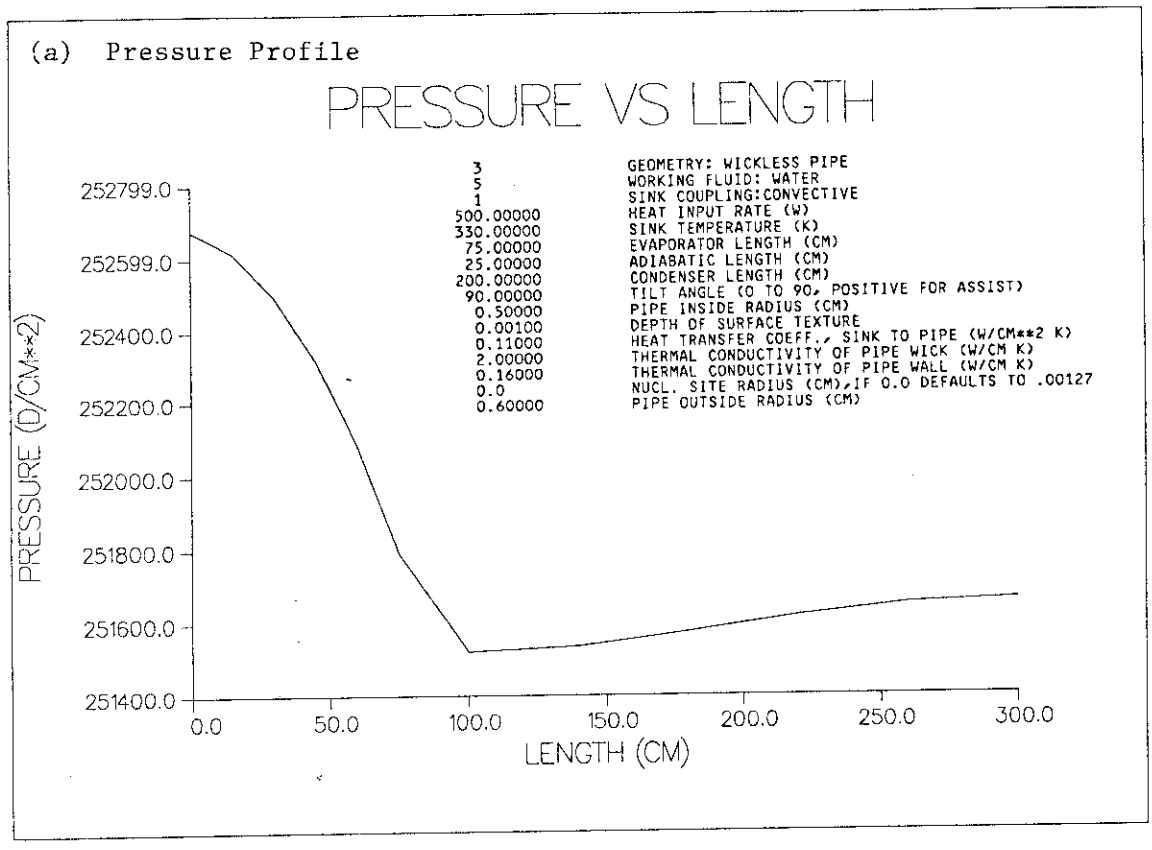

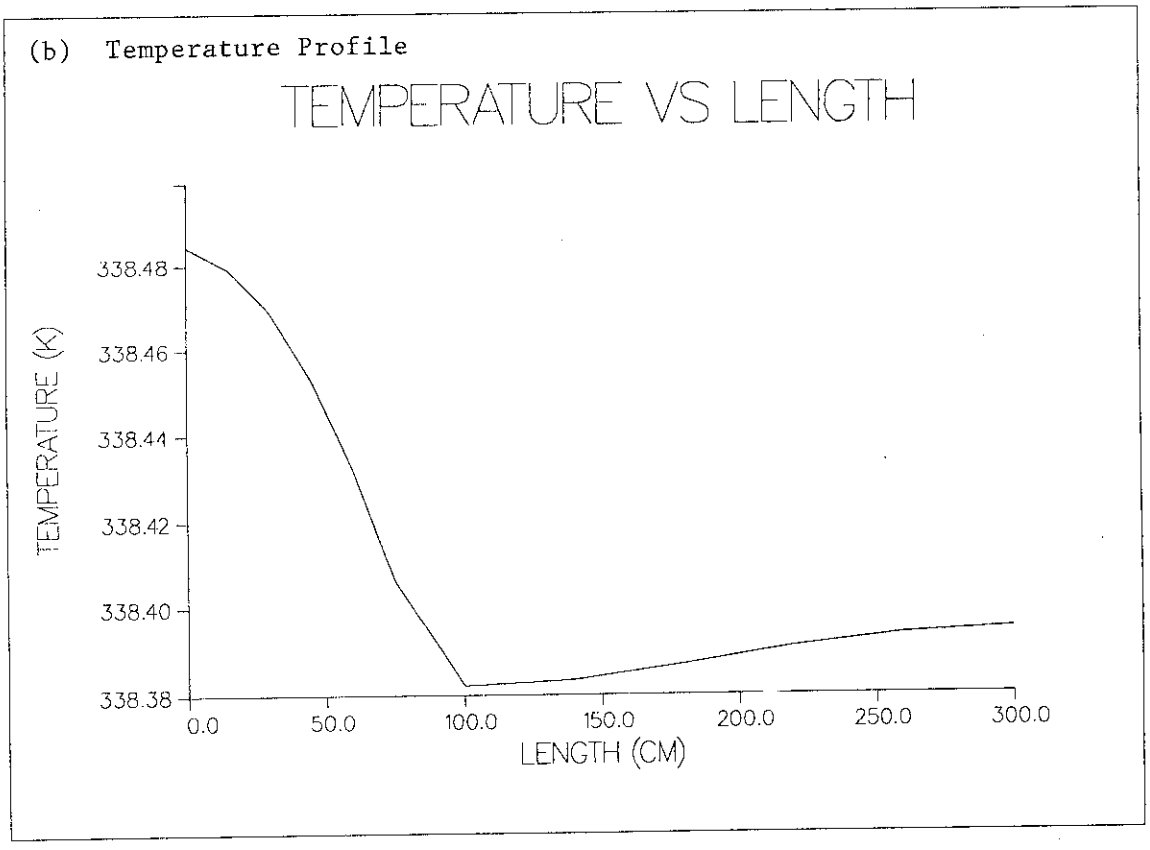

Fig. 16 Pressure and Temperature Profiles in the Long Wickless Heat Pipe (Input Power 500 W, Sink Temperature 330 K)

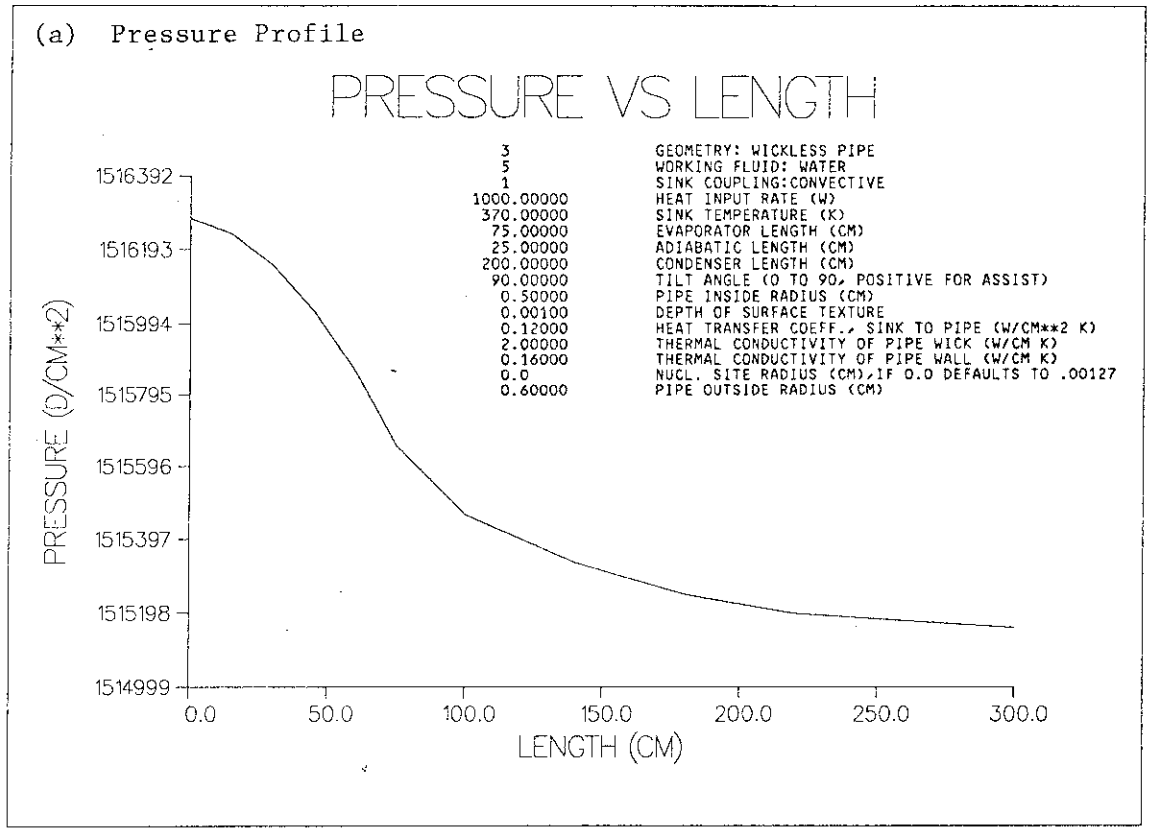

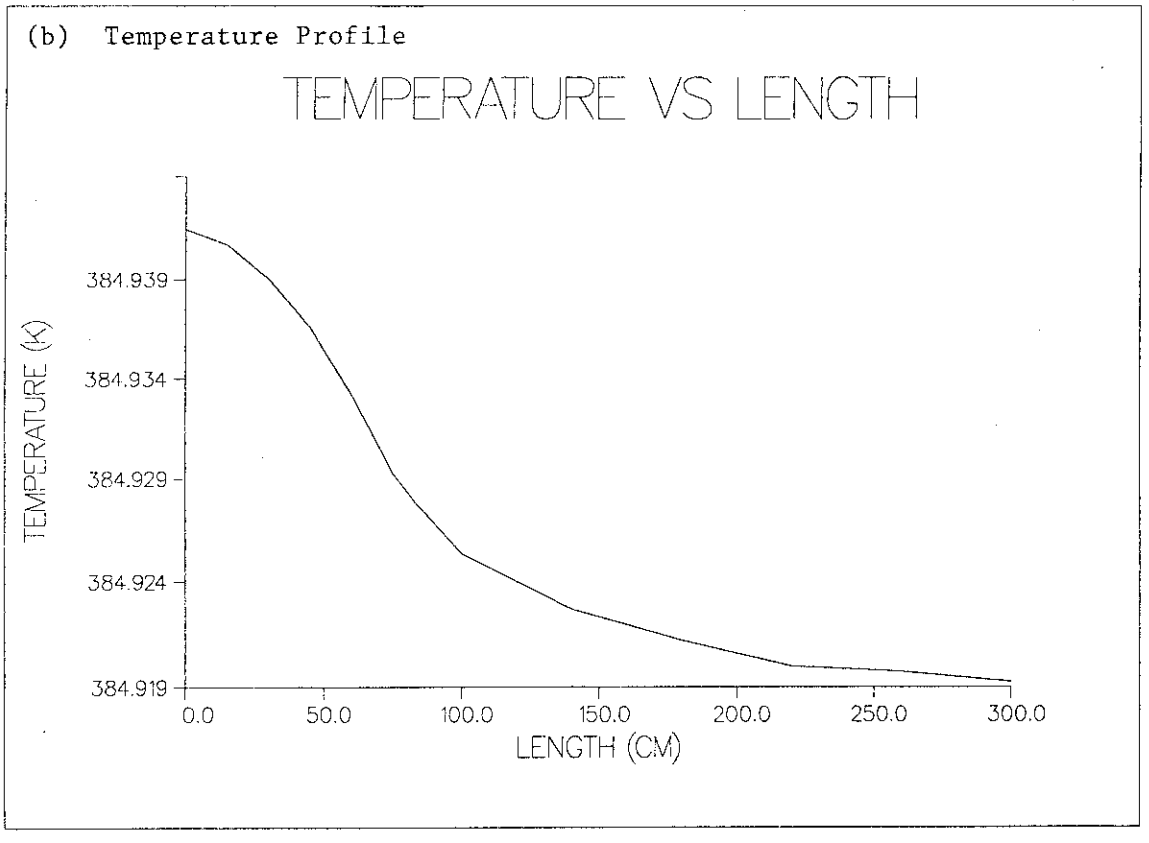

Fig. 17 Pressure and Temperature Profiles in the Long Wickless Heat Pipe (Input Power 1000 W, Sink Temperature 370 K)

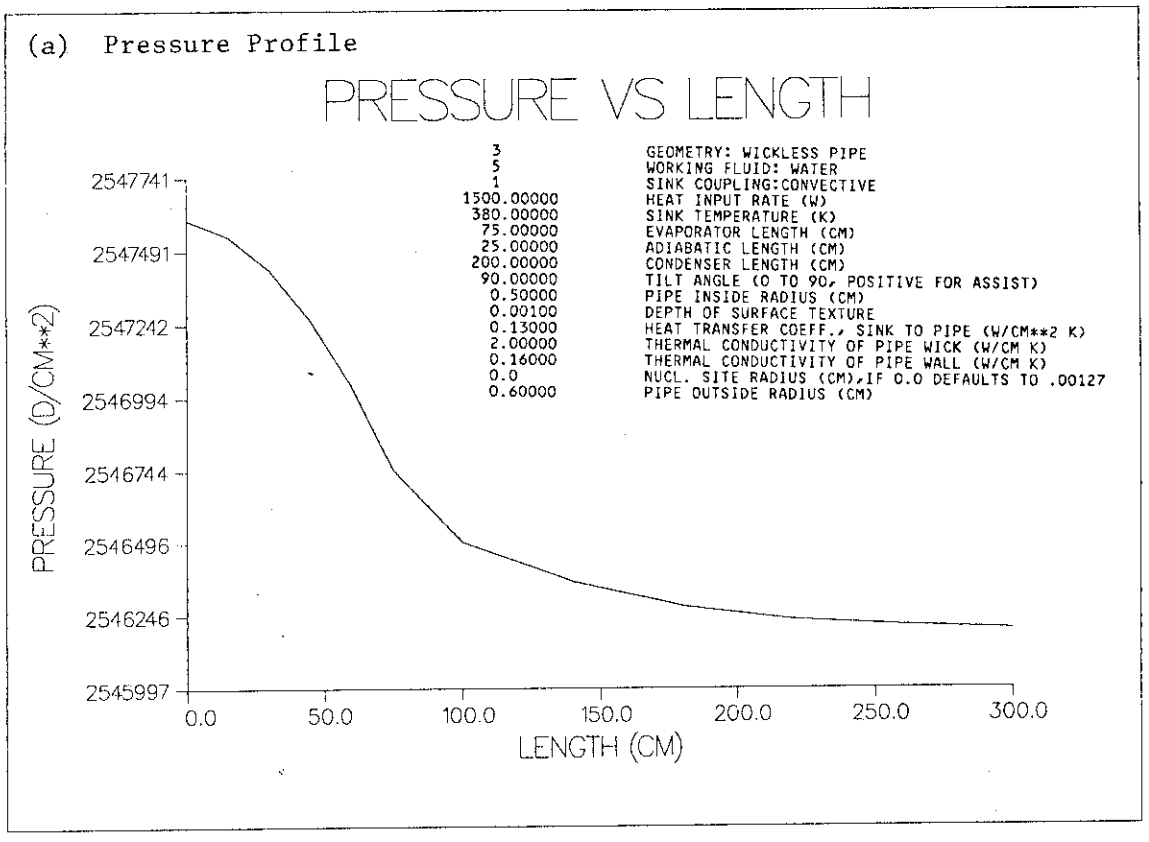

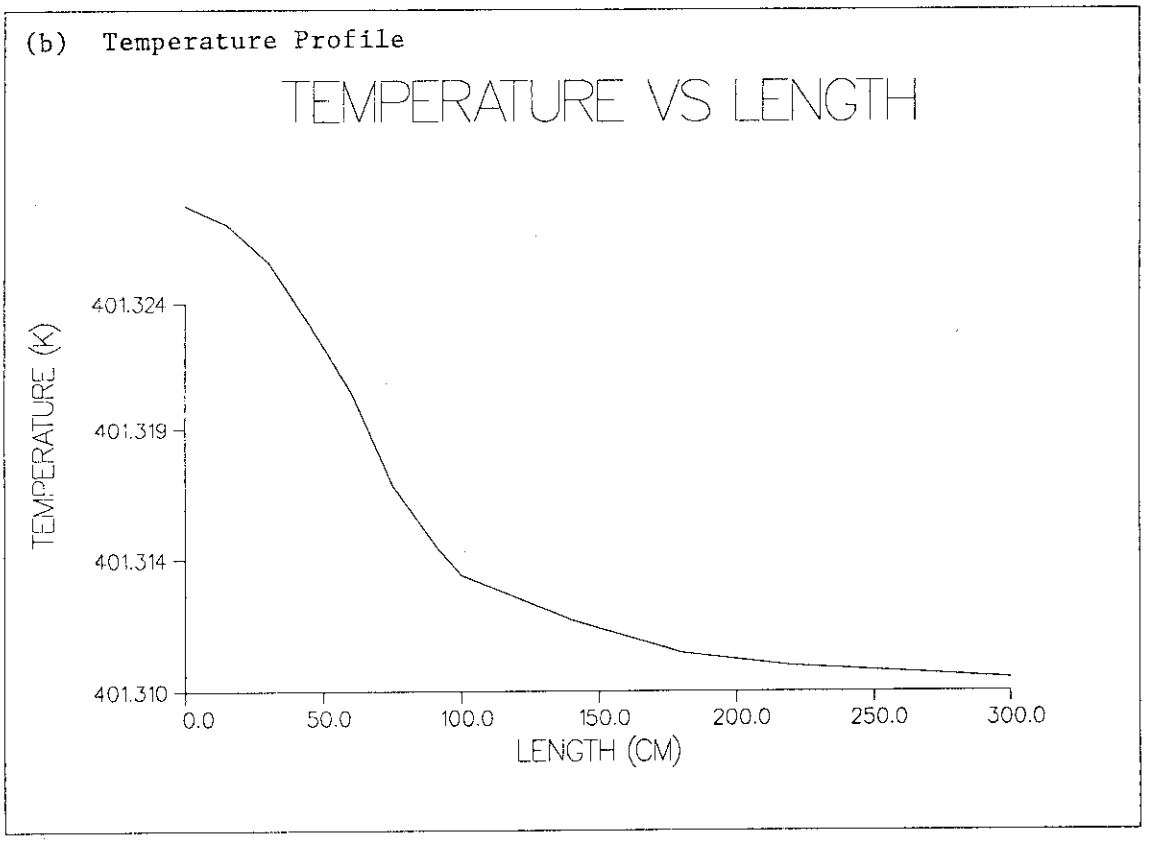

Fig. 18 Pressure and Temperature Profiles in the Long Wickless Heat Pipe (Input Power 1500 W, Sink Temperature 380 K)

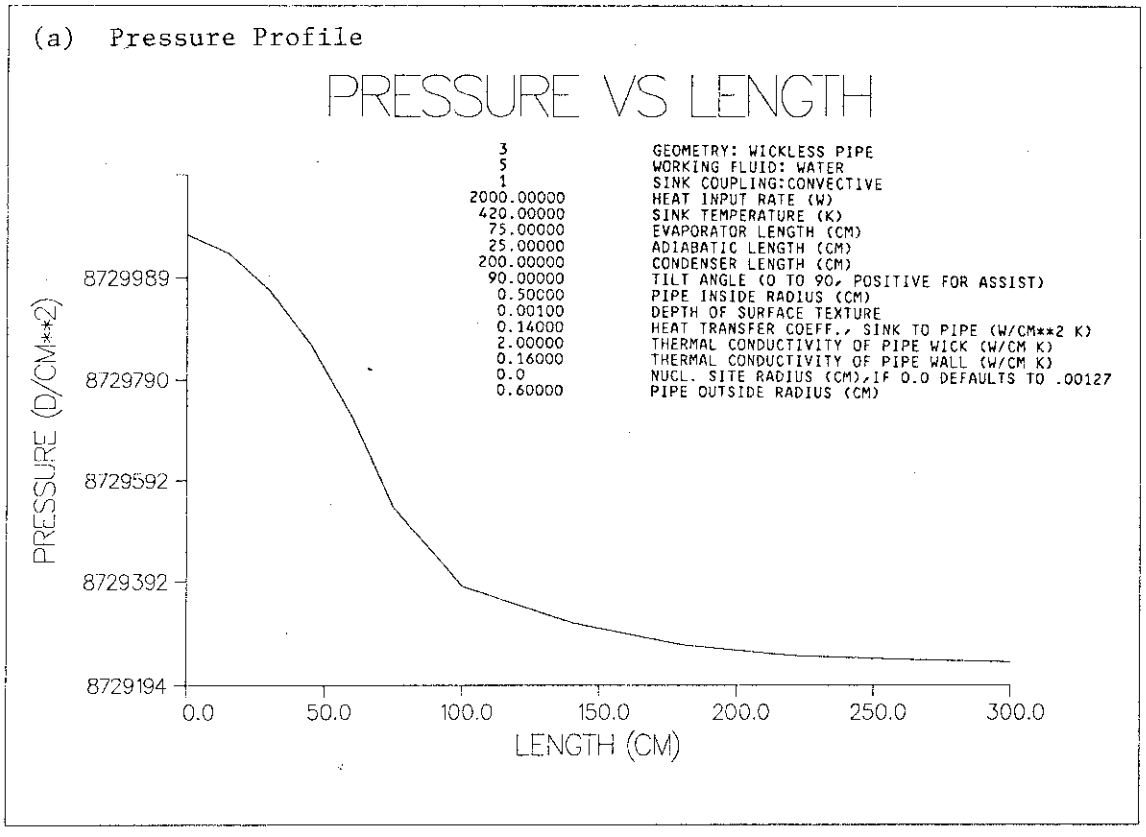

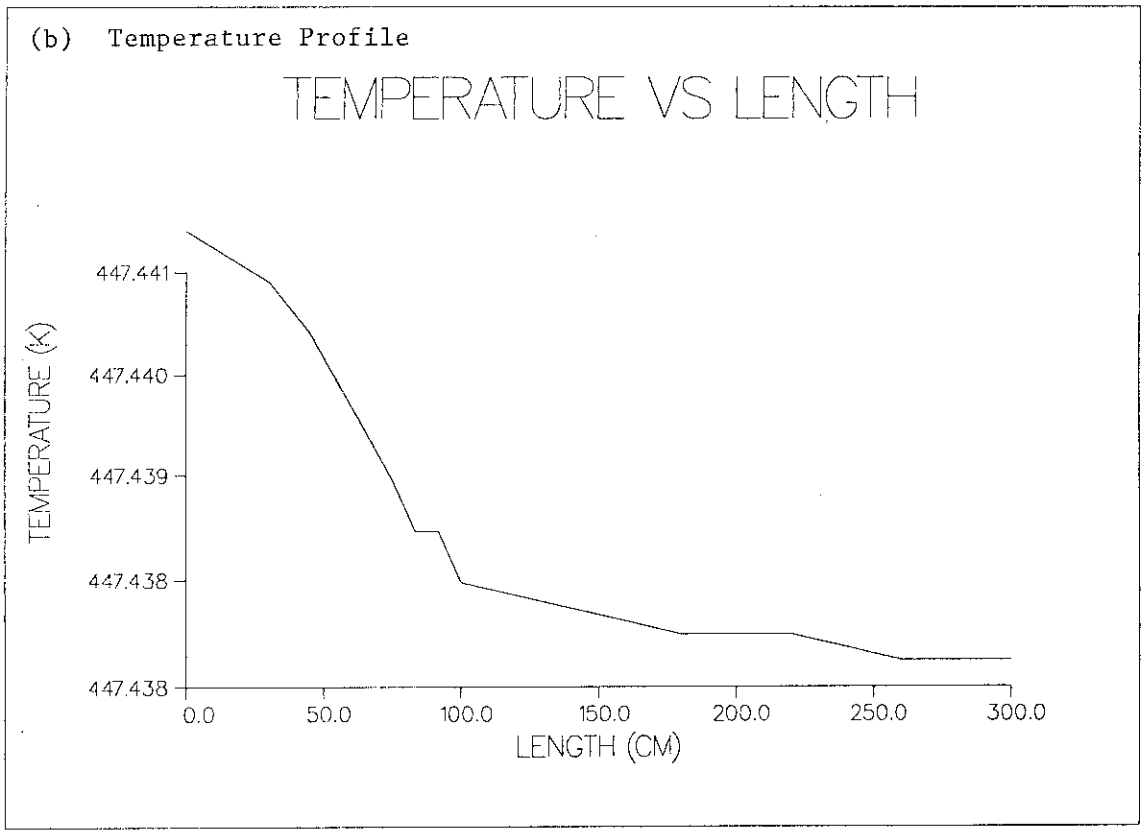

Fig. 19 Pressure and Temperature Profiles in the Long Wickless Heat Pipe (Input Power 2000 W, Sink Temperature 420 K)

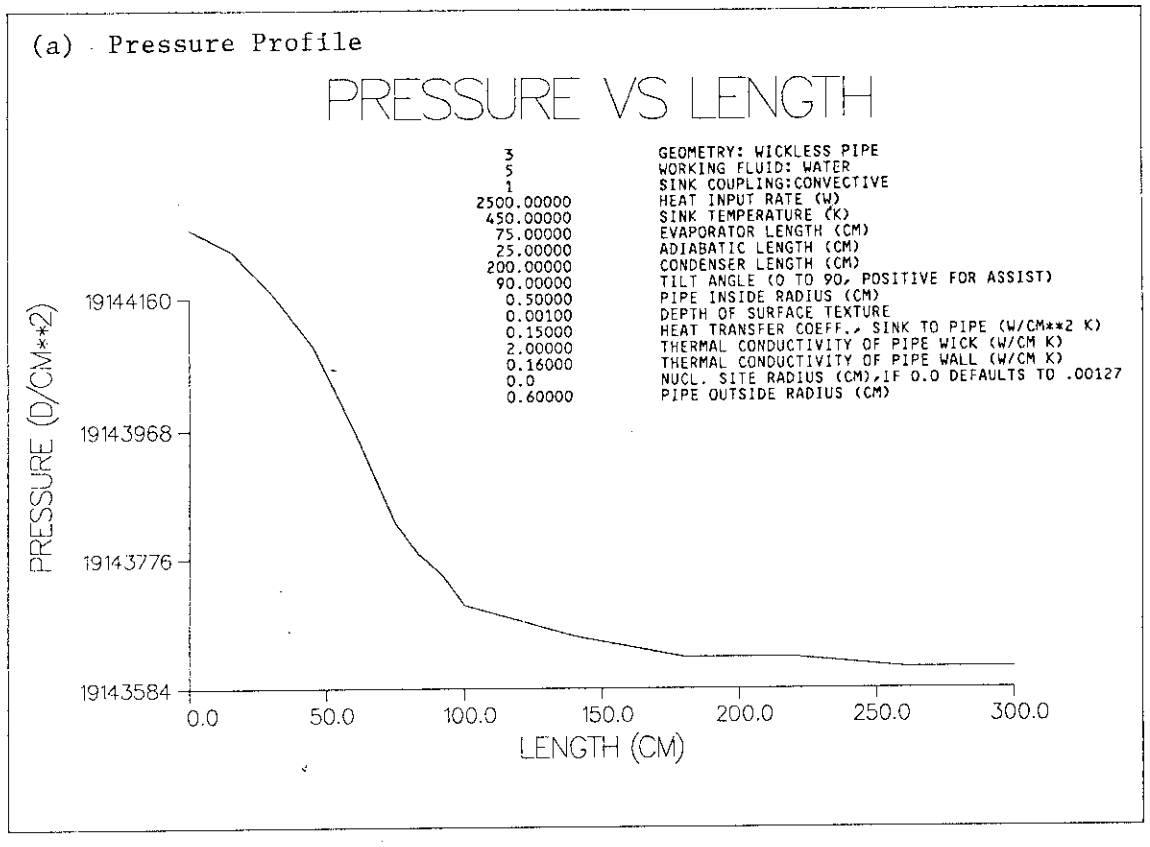

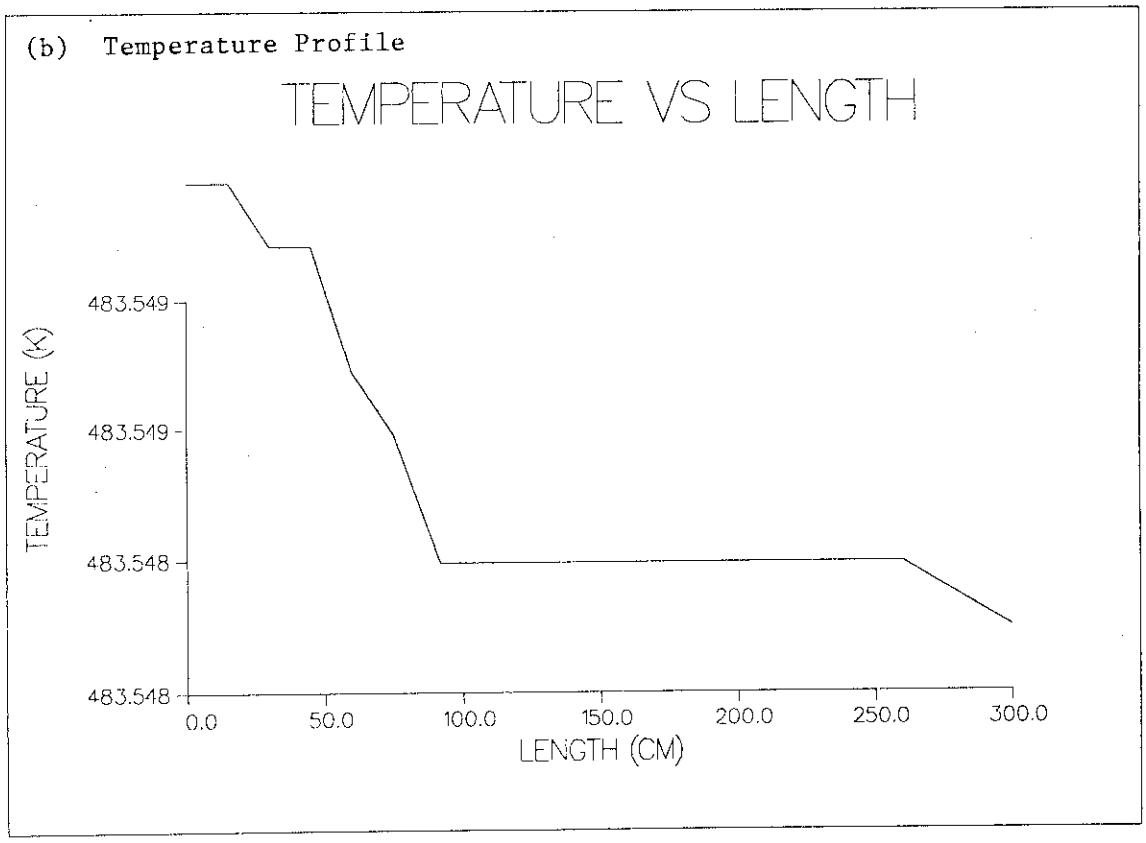

Fig. 20 Pressure and Temperature Profiles in the Long Wickless Heat Pipe (Input Power 2500 W, Sink Temperature 450 K)

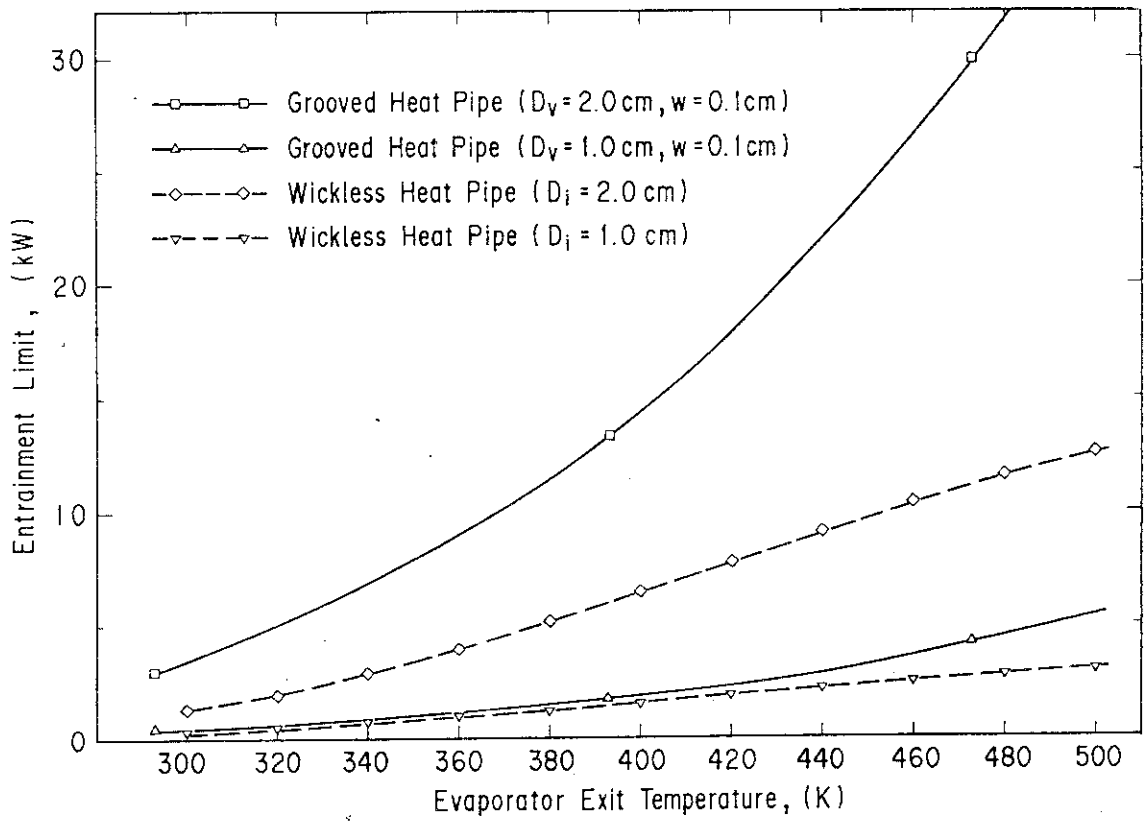

Fig. 21 The Difference of Entrainment Limits between the Grooved Heat Pipe and the Wickless Heat Pipe

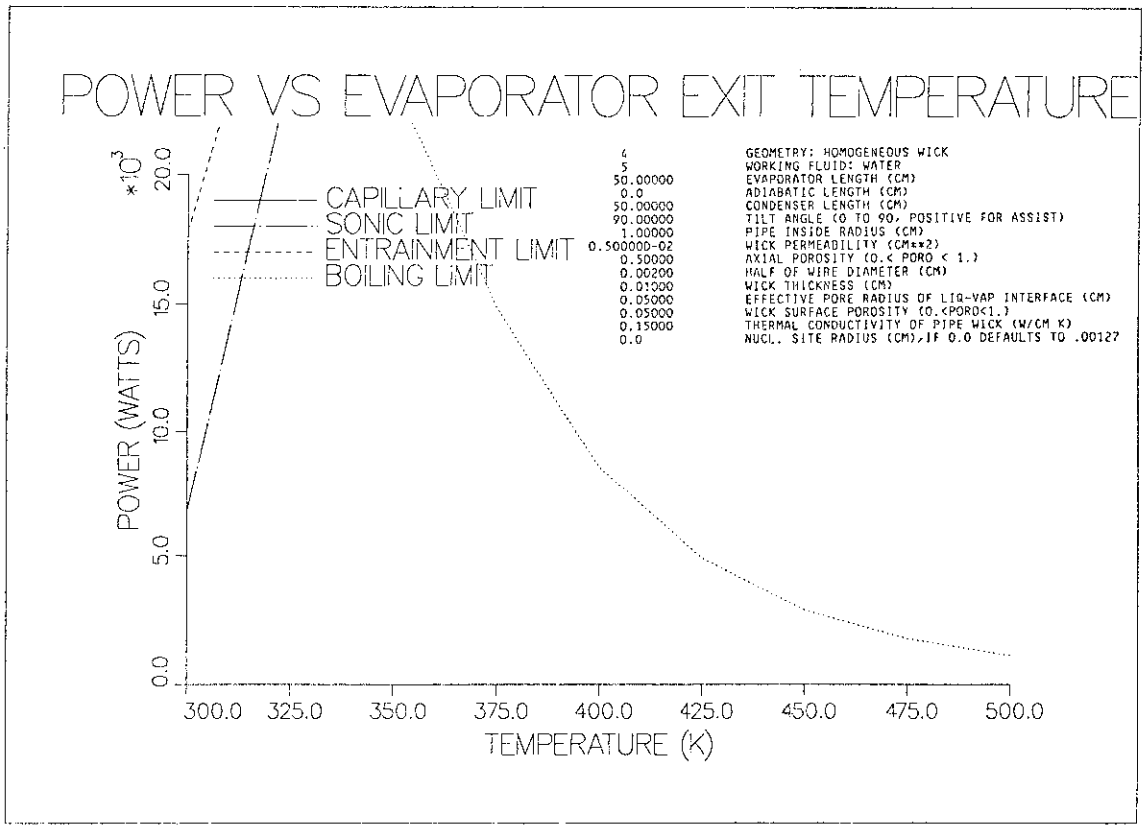

Fig. 22 Power Limits of the Homogeneous Wick Heat Pipe

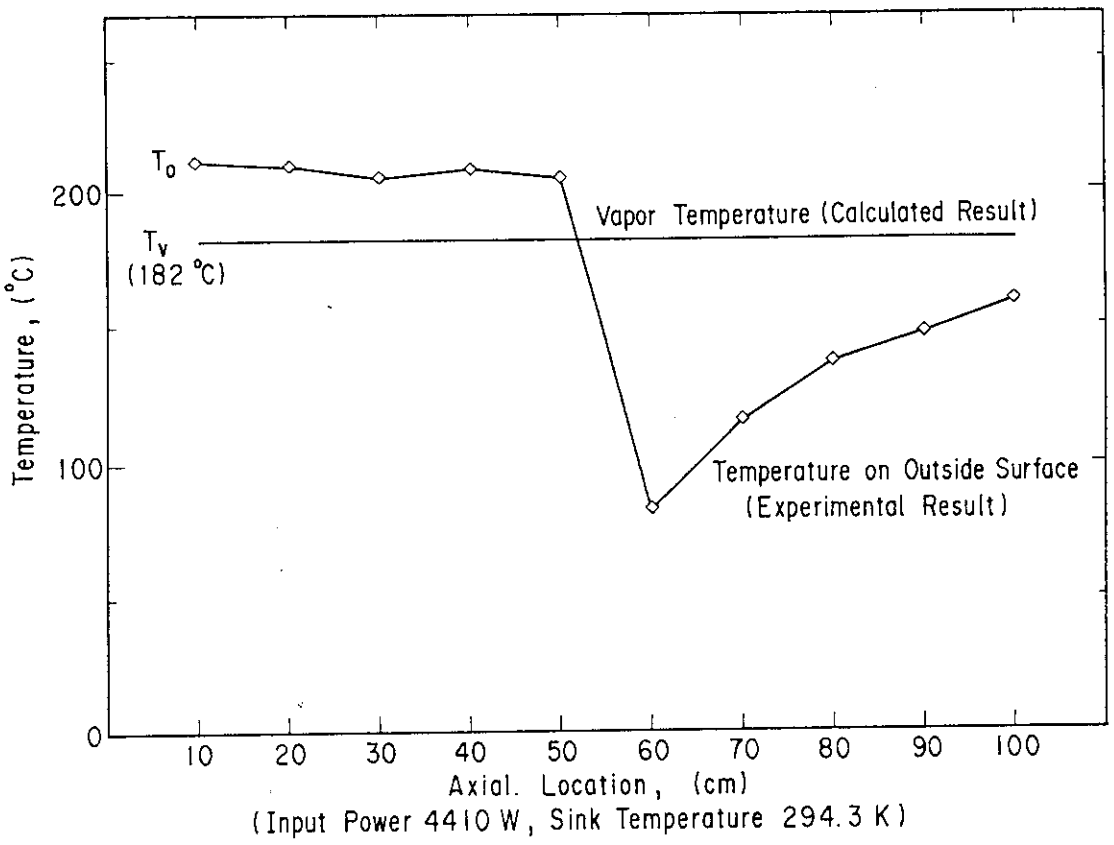

Fig. 23 The Profiles of Vapor Temperature and Outside Surface Temperature of the Wickless Heat Pipe
(Input Power 4410 W, Sink Temperature 294.3 K)